Instrumentation Project Final Report

Curtiss Melder
University of Utah
(Dated: May 11, 2007)

I. INTRODUCTION

The instrument built for this project is used to measure rubidium vapor density in glass cells. The research group run by Brian Saam is actively researching the properties of hyperpolarized noble gasses. The process used by the group to produce the hyperpolarized gas is known as spin exchange optical pumping (SEOP). Rb vapor is part of the SEOP process, and knowing the correct Rb vapor density is a crucial component in producing high percentages of hyperpolarized noble gasses.

This project is a continuation of a project started by Ryan May while working for Brian Saam in 2006. The fundamental principle upon which Rb vapor density is measured, is Faraday rotation. The amount of rotation of the polarized light is a function of the rubidium vapor density. Therefore the vapor density can be measured by measuring the polarization rotation angle induced by the rubidium cell. For magnetic fields ranging from 10-60 gauss, typical rotation angles are 6-14 mrad. The previous instrument relied on a rotation stage with resolution of ~0.6 mrad to make these measurements. As Ryan demonstrated, this method works, however, it also attests to the skill involved in making the difficult measurement.

Killian empirically determined a formula that describes the saturated vapor pressure of Rb as a function of temperature (7). However, many groups have measured the Rb vapor density in cells, and have found the Rb density to vary from cell to cell. They have also noted, that in some cases the Rb vapor density has varied from the Killian curve, by as much as a factor of 2. The goals of this project were to make a reliable instrument for measuring Rb vapor density, check for cell to cell variation, compare the cells to the Killian curve, check for hysteresis caused by either magnetic field fluctuations, or by temperature fluctuations, and to observe cell variations over long periods of time.

To accomplish these goals, this project has some additions to the one completed by Ryan. These additions include

- A photoelastic modulator (PEM).
  - Additional optics used with the PEM.
  - Lock-in amplifier.
- A summing Circuit.
- A power supply for the photodiode detectors.
- Additional shim coils for 3rd axis.
- Instrument rigidification.

Section II of this report will cover Faraday rotation and how it is related to the Rb vapor density. Section III will give a detailed description of the instrument. It will also discuss the polarization states of the light, and how the PEM significantly increases the signal to noise ratio of the system. Section IV will show data and results, and compare them to the expected values from the Killian vapor density curve. Section V is the conclusion.

II. FARADAY ROTATION AND Rb VAPOR DENSITY

A. Faraday Rotation

Faraday rotation was first observed by Michael Faraday in 1845. What he observed, was that as light propagated in a dielectric material, collinear to a magnetic field, the plane of vibration of the electric field rotated [1]. The rotation is described by equation 1,

$$\theta = VBl \qquad \text{eq. (1)}$$

where θ is the rotation angle of the E-field, B is the magnetic field strength, l is the length traversed by the light, and V is the Verdet constant. The Verdet constant is particular to the material the light is propagating through.

The following description uses classical mechanics to describe the cause of Faraday rotation. As the oscillating E-field of linear polarized light propagates through a medium, it causes the electrons to oscillate in the same plane as the E-field. When this is done in the presence of a magnetic field that is collinear with the light, the electrons vibrate in a direction perpendicular to the B-field. Because the electrons are vibrating in a direction perpendicular to the magnetic field, they experience a force known as the Lorentz force. This force is described by equation 2 (3).

$$F = qE + qv \times B \qquad \text{eq. (2)}$$

The cross product term of the Lorentz force is felt by the electron in a direction perpendicular to both the propagation of light, and the direction of vibration. The result is, the polarization angle of the light is rotated as it passes through a medium collinear with a magnetic field.

B. Rb Vapor Density

As discussed earlier, Rb vapor can be used as a medium for inducing Faraday rotation. The relationship between the amount of rotation and the Rb vapor density is described by equation 3, and table 1 is a listing of the constants and units used in equation 3 (8).

$$\theta = [Rb]\frac{le^2\mu_B B}{18mhc}\left(\frac{4}{\Delta^2_{1/2}} + \frac{7}{\Delta^2_{3/2}} - \frac{2}{\Delta_{3/2}\Delta_{1/2}}\right) \qquad \text{eq. (3)}$$

Parameter/Constant	Value	Units
θ	Measured	Radians
[Rb]	Solved for	cm^{-1}
length l	Measured	cm
electron charge e	4.802e-10	esu
Bohr magneton μ_B	9.274e-21	$erg * gauss^{-1}$
magnetic field B	Measured	$gauss$
electron mass m	9.1095e-28	g
Planks constant h	6.6262e-27	$erg *$ sec
speed of light c	2.998e10	$cm * s^{-1}$
Detuning from D1 resonance $\Delta_{1/2}$	Measured	Hz
Detuning from D2 resonance $\Delta_{3/2}$	Measured	Hz

Table 1 Table of values used to solve the rubidium vapor density.

The D1 resonance corresponds to electrons transitioning from the $5P_{1/2} \rightarrow 5S_{1/2}$ state. The D2 resonance corresponds to electrons transitioning from the $5P_{3/2} \rightarrow 5S_{1/2}$ state. The D1 and D2 resonance lines for Rb occur at 795 nm and 780 nm respectively. Equation 3 shows that at D1 and D2, the rotation goes to infinity, and that far away from either of the two resonance lines, results in very little rotation. The laser for this instrument was tuned to 779.5 nm, or in other words $\Delta_{3/2} \approx 2.47e11Hz$. After measuring

θ, l, B, $\Delta_{1/2}$, and $\Delta_{3/2}$, the only unknown is the rubidium vapor density [Rb], which is solved for.

III. INSTRUMENT DESCRIPTION

The instrument can be divided into three main parts, the probe beam optics, the magnetic coil and oven assembly, and the detection optics as shown in Figure 1.

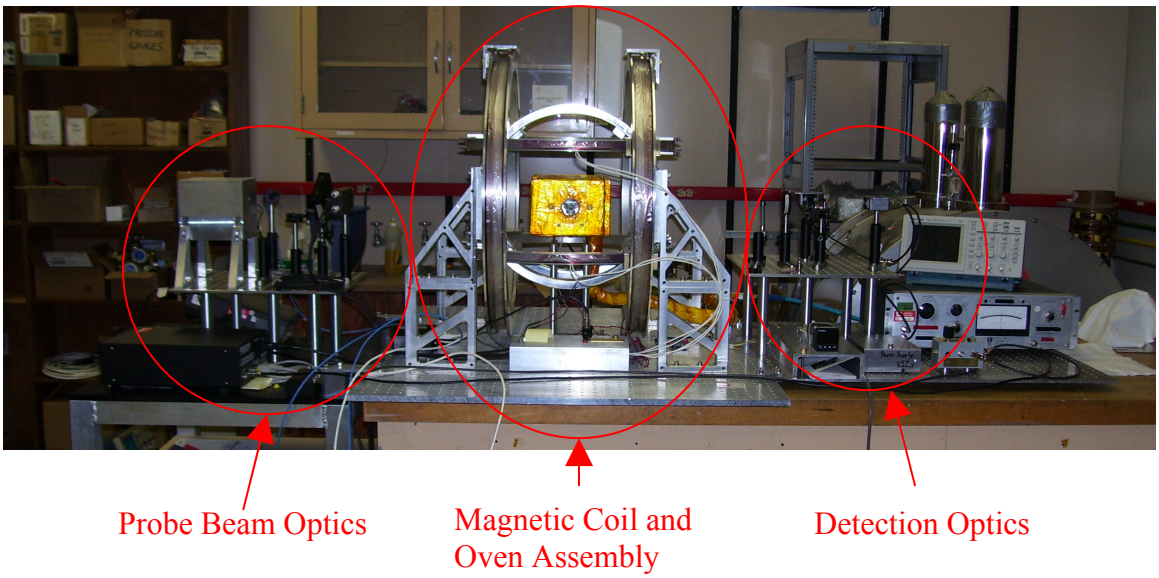

Figure 1 Setup of the entire instrument.

A. Probe Beam Optics

The probe beam optics consists of a temperature controlled extended cavity diode laser (ECDL), glass plate, Ocean Optics spectrometer, quarter waveplate, and a photoelastic modulator as shown in Figure 2.

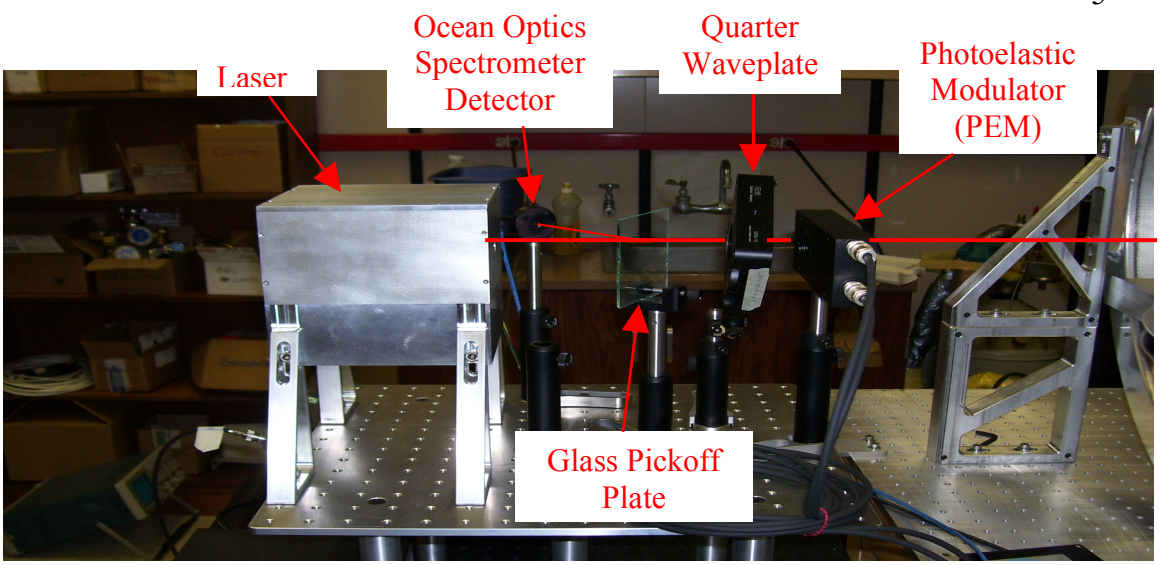

Figure 2 Optical components on the probe beam optics table.

The ECDL and the temperature controller was built by Ryan May. The front and top views of the laser are shown in Figures 3 and 4.

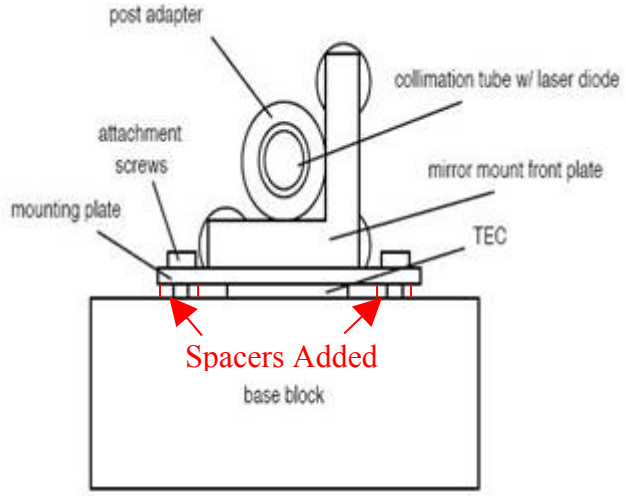

Figure 3 Front View ECDL (modified from (2))

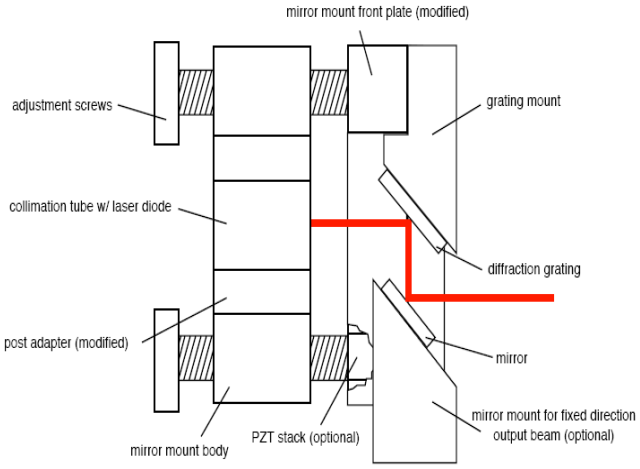

Figure 4 Top View ECDL (2)

The extended cavity is composed of a diffraction grating and a mirror. The details of the grating equation and how the ECDL works is covered in Ryans report, and will not be covered here. However, it is important to note that the ECDL accomplishes two things, first, it narrows the line width to about 0.1nm, and second, it provides a mechanism to adjust the lasing frequency. The ECDL can do this because the grating can be rotated independent of the laser about two axes. It can be rotated about a vertical axis, and about

a horizontal axis that is perpendicular to the laser beam. Rotation about the horizontal axis allows for proper alignment of the reflected 1st order beam back into the laser. This adjustment is made by adjusting the top knob shown in Figure 3. If the laser is unstable, this knob may need slight adjustment. Adjustment of the knob on the lower end of the "L" in figure 3 causes the diffraction grating to rotate about a vertical axis. This adjustment causes the lasing line to shift, thus enabling the laser to be tuned to 779.5 nm.

One of the goals of the project was to rigidify the setup. With that in mind, there were some additions or modifications made to the laser assembly. As shown in Figure 3, spacers that fit around the attachment screws and between the mounting plate and base block were added. Without these spacers it was impossible to securely fasten the laser to the base block without causing the mounting plate to bow over the TEC. If the mounting plate were allowed to bow over the TEC, then it would not maintain good thermal contact, and temperature control of the laser would be compromised. Also, an additional screw was added to the bracket holding the output mirror of the ECDL. Using two screws ensured that the bracket could not wobble or pivot.

Another modification was made to the base block. Previously, the shear size and mass of the base block was used to keep it in one place. It sat flat on the optic table without being fastened down in anyway. In the current setup it was necessary to raise the level of the laser. Brackets were designed to raise the level of the laser, to rigidly hold the laser block, and to provide for adjustment both vertically, and horizontally side to side. This assembly is shown in Figure 5.

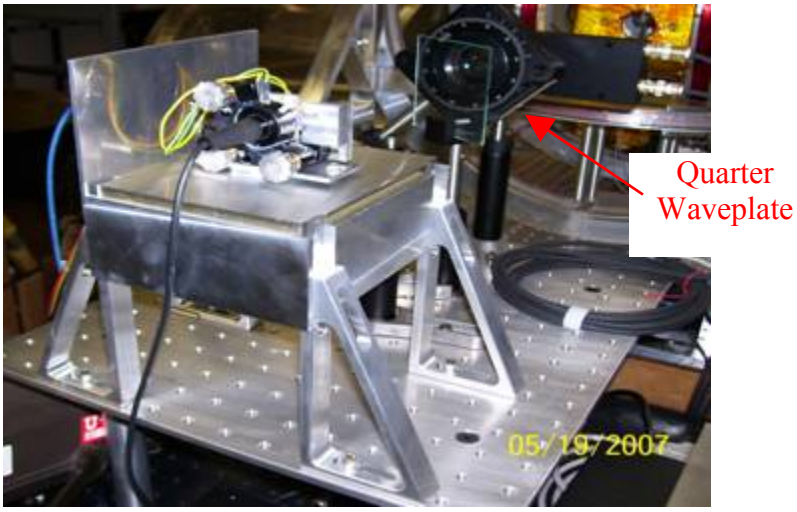

Figure 5 Laser mount and bracket assembly ensure rigid structure for improved laser stability while maintaining adjustability.

One more change to the laser assembly was the addition of a cover shown in Figure 2. Without the cover, small air currents in the room, or even standing near the laser caused the temperature to fluctuate ~ ±0.06º C. These small fluctuations caused the output power of the laser to fluctuate as well. With the cover, the laser temperature fluctuates a maximum of ±0.01º C, which is also the maximum temperature resolution of the controller.

The glass plate is used to pick off a small portion of the beam, and reflect it back into the Ocean Optics spectrometer. The Ocean Optics spectrometer provides real time information about the emitted wavelength of laser light. This is useful both for adjusting the extended cavity, and while making measurements to ensure the laser line is where it is expected to be.

The 780 nm multiorder quarter waveplate shown in Figure 5 converts the vertical linear polarized light emitted from the laser into circular polarized light. To accomplish this, the fast and slow axes of the quarter waveplate are oriented at +45º for one axis, and -45º for the other axis relative to the vertical polarized laser light. Using the setup below in Figure 6, the circular polarized light was analyzed to determine how circular it was.

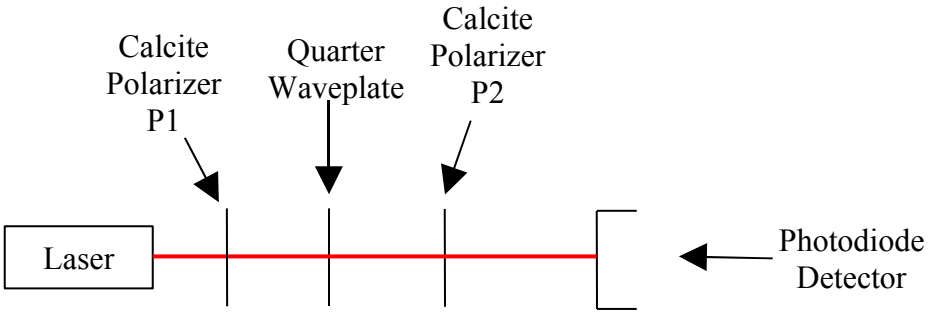

Figure 6 Analyzer setup used to ensure good circular polarization after the quarter waveplate.

The best results gave ~20%-25% variation in intensity as the calcite polarizer was rotated. A significant portion of this variation was caused by the error inherent in the 780 nm multiorder quarter waveplate. To compensate for this error, the quarter waveplate was mounted on a post at a 45º angle as shown in Figure 5. Next, the waveplate was rotated about the mounting post. This effectively lengthens the optical path length of the

axis that is positioned perpendicular to the axis of rotation. This slight rotation can be seen in Figure 2. With P1, the variations were reduced to 1.7%, and without P1, the variations were reduced to 14%.

The last component on the probe beam optics table is the photoelastic modulator (PEM). This PEM is a series I/FS50 and was purchased from Hinds Instruments. It has a nominal operating frequency of 50 kHz, and a useful aperture of 16 mm. This PEM head has the noninterference option (NIO) as well as the magnetic field compatibility option (MFC). The optical head is a resonant device composed of two components, the optical element, and the transducer, as shown in Figure 7.

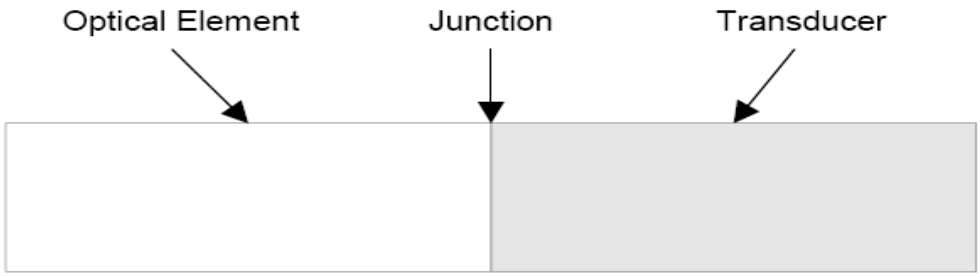

Figure 7 Optical Head For PEM (4)

The optical element is composed of birefrigent fused silica. The amount of birefringence, or in other words, the amount of retardation between the slow and fast axes is a function strain, either in compression or tension. The transducer produces this strain in the fused silica sinusoidally on resonance at 50 kHz. The result is a retardation that can be described by equation 4, where β is the depth of retardation.

$$\delta = \beta * \sin(\omega t) \qquad \text{eq. (4)}$$

The PEM is set up on this instrument with the fast or slow axes, oriented either vertically or horizontally. For circular polarized light incident on the PEM, the resulting transmitted light is elliptically polarized with the semimajor axis oscillating between ±45º. Equation 5 shows that α always equals 45º regardless of the retardation δ, as long as $E_{ox} = E_{oy}$, where E_{ox} and E_{oy} are the amplitudes of the electric field in their respective directions. Also, in the special case where $E_{ox} = E_{oy}$, the angle α changes instantaneously from positive to negative as the polarization passes through circular. Changing the retardation only affects the eccentricity of the ellipse with the two extreme

cases being a circle or a line. This is the dynamic polarization state of the light as it enters the magnetic coil and oven assembly.

$$\tan 2\alpha = \frac{2E_{ox}E_{oy}\cos\delta}{E_{ox}^2 - E_{oy}^2} \qquad \text{Eq. 5 (1)}$$

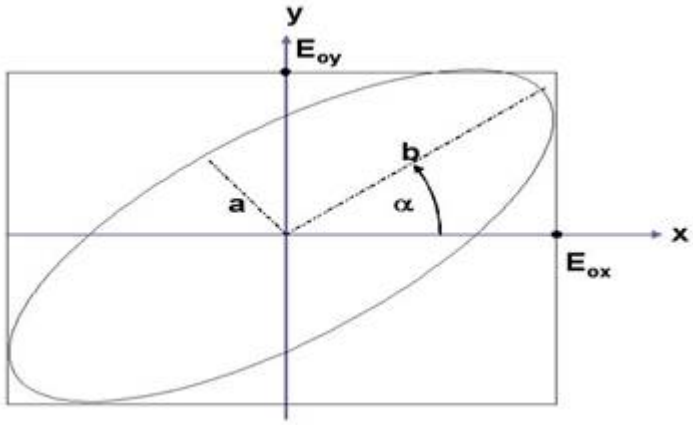

Figure 8 Orientation of semimajor axis. Refer to Equation 5 (5).

B. Magnetic Coil and Oven Assembly

The coil assembly consists of three sets of coils, the main field coils, and a horizontal and vertical set of shim coils as shown in Figure 9.

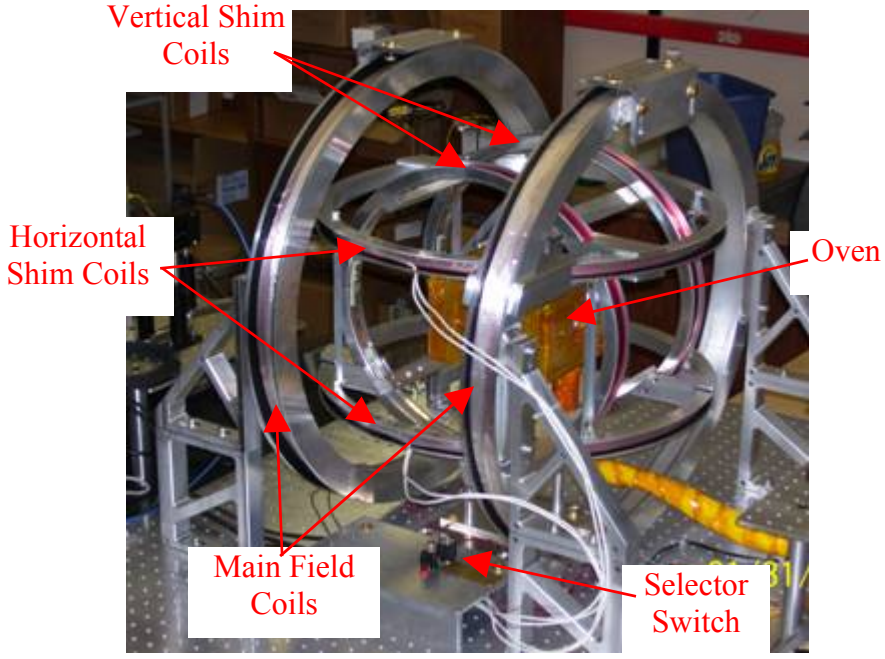

Figure 9 The 3D magnetic field coil assembly gives precision control over the field conditions inside the oven.

The main coils are rigidly supported by brackets as shown in Figure 9. The shim coils are nested inside of each other while maintaining the Helmholtz coil configuration. Each smaller set of coils is rigidly fastened to the directly bigger set of coils using interconnecting brackets. Therefore in this configuration, all three sets of coils are all fastened together into one integral unit.

The shim coils are used to shim out the Earth's magnetic field. They are positioned vertically and horizontally to compensate for both the vertical and horizontal components of the Earth's field. The instrument is set up with the main field oriented in an east-west direction. There is essentially no component of the Earth's field in this direction. Therefore in theory, zero magnetic field is attainable in the center of the oven.

Each set of coils has its own power supply. The shim coils are wired in series, and the main field coils are wired in parallel. The only reason the main fields are wired in parallel, is because that is the only configuration our power supplies could accommodate. The main field coils required two power supplies. They are connected together in a master-slave configuration. Therefore, to make current adjustments, it is necessary to turn only one knob on the master power supply. The current for each set of coils runs through a power resistor located near the selector switch shown in Figure 9. Because the voltage across the resistor is proportional to the current running through it, and because the current running through the coil is directly proportional to the magnetic field produced by the coil, the voltage across the resistor is also proportional to the magnetic field. The relationship of magnetic field and voltage across the resistor is shown for each of the coils in Figure 10.

The field of each coil was measured in the center of the oven, where the Rb cell sits, using a F.W. Bell model 5070 Gauss/Teslameter Hall effect probe. The voltage across each power resistor was measured using a digital multimeter. Each coil can be selected individually using the selector switch shown in Figure 9. Using the plots in Figure 10, the shim coils were adjusted to compensate for the Earth's magnetic field.

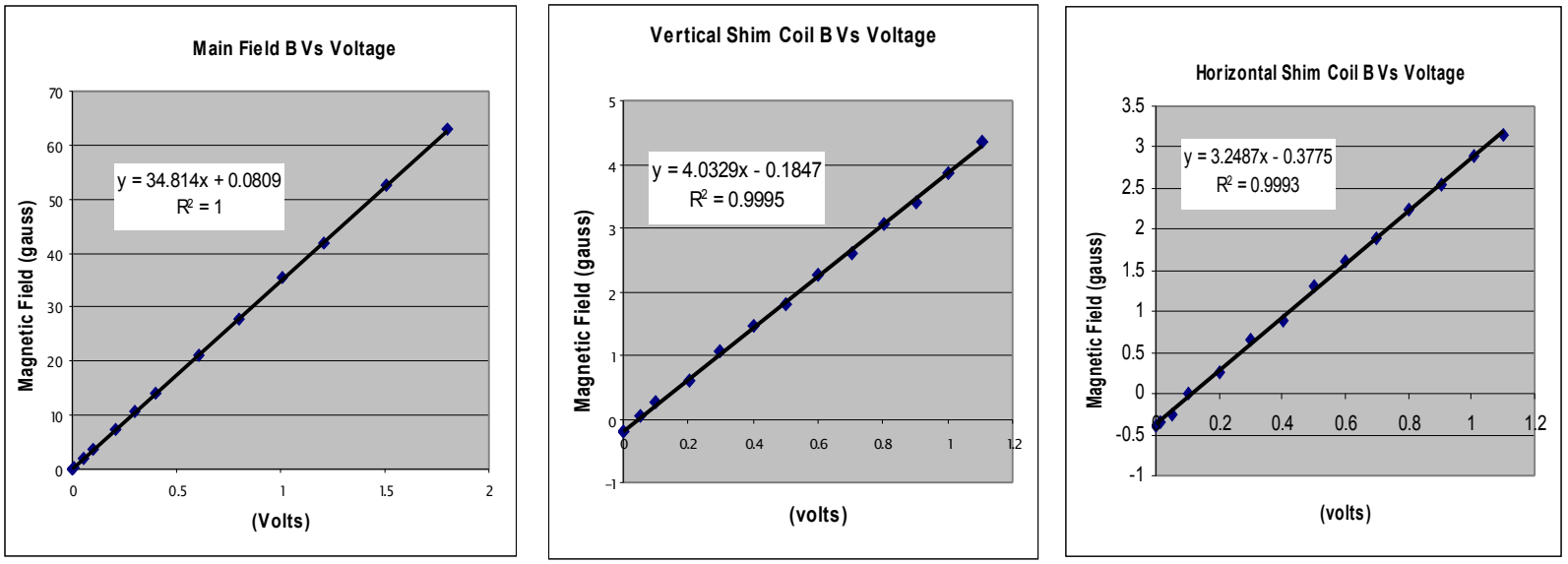

Figure 10 Relationship of magnetic field and voltage across a power resistor for each set of magnetic field coils. The equation for the main field line was use in calculating the magnetic field strength during the Rb vapor density measurements.

The oven assembly is essentially the same as what Ryan previously used with a few modifications. The air inlet was modified to fit this particular coil arrangement. Two vent holes were added to the top, and an extra window was added for the option of using a transverse probe beam for polarimetry experiments. The Rb cell sits in the oven as shown in Figure 11.

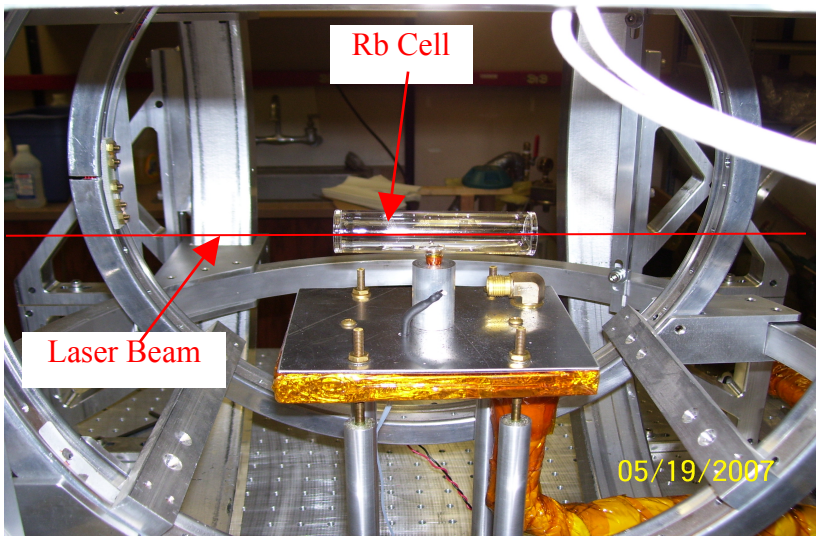

Figure 11 Rb cell shown sitting in the oven without the oven cover.

C. Detection Optics

The detection optics consists of a 780 nm multiorder half waveplate, a polarizing beam splitting cube, and two photodiode detectors as indicated in Figure 12.

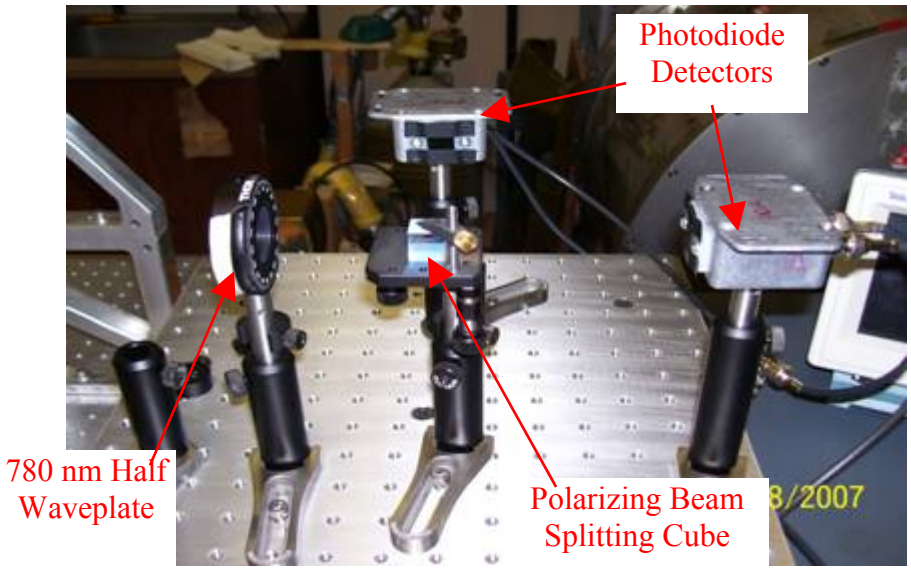

Figure 12 Detection optics consist of a half waveplate, a polarizing beam splitting cube, and two photodiode detectors.

The half waveplate is used to rotate the polarization of the laser beam. This can be used to "zero" the system before taking a measurement. The polarizing beam splitting cube (pbc) reflects the vertical polarization and transmits the horizontal polarization. The photodiode detectors can then be used to individually analyze the vertical and horizontal polarization states. Previously there was a lens positioned before the half waveplate that was used to focus the beam onto the photodiode detectors. However, it was discovered that because of inhomogeneities in the photodiode, a broader beam gives a better response than a pinpoint beam.

D. Theory of Operation

This portion of the report will discuss in detail the polarization state of the light as it propagates through the system, and it will look at how the signal is interpreted and processed. Refer to the block diagram in Figure 13.

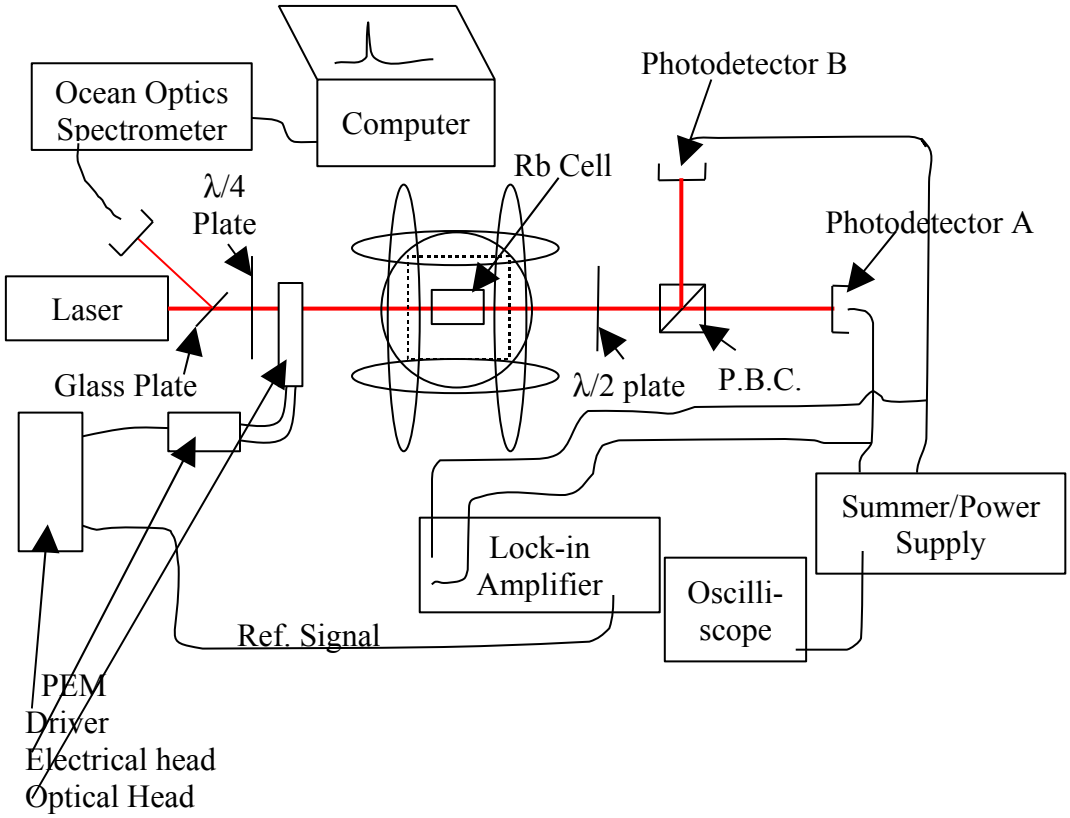

Figure 13 Block Diagram of Instrument (top view).

As previously discussed, the initial polarization of the laser beam is linear and oriented vertically. The quarter waveplate is oriented such that it converts the linear polarized light into circular polarized light. After exiting the PEM the light is elliptically polarized with the semimajor axis oscillating sinusoidally between ±45º. If the oven and cell were removed from the system, then the light would propagate, without being rotated, through the half waveplate and into the polarizing beam splitting cube p.b.c. The p.b.c then separates the vertical and horizontal polarization components sending them into photodetector B (PDB) and photodetector A (PDA) respectively. In the case where there is no rotation, e.g. the oven and cell are not present, and the half waveplate is properly oriented, the difference of PDA and PDB is equal to zero. This can be seen by inspection in Figure 14, that when α=45º, and θ=0º, then there are equal E-field components in the X and Y directions. However, with the magnetic field turned on, and the Rb cell and oven in place, the Rb vapor causes the polarization of the light to rotate according to equation 3. It is important to note, that this rotation does not change the angle α, rather the whole reference frame is rotated by θ. This is shown in Figure 14.

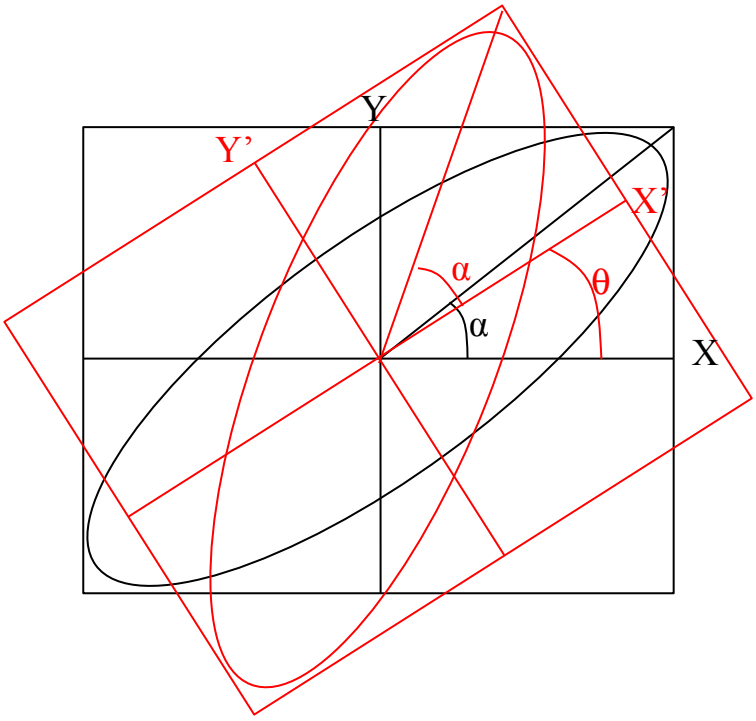

Figure 14 Ellipse rotation diagram illustrating the effect of rotation. When θ = 0, there are equal components of the E-field in the X and Y directions. However, when θ ≠ 0, then the E-field seen in the X and Y directions oscillates at the PEM frequency.

The PEM causes the polarization to morph from an ellipse with some maximum eccentricity with the major axis at 45º, into a circle, and then back into an ellipse with the major axis at -45º. This is still the case after the polarization has been rotated, except that now the major axis is rotated at ±45º relative to the X' axis. This results in a oscillating signal seen by the two photo detectors that are still in the initial X-Y reference plane. The oscillating signal from PDA and PDB is sent to the lock-in amplifier. The lock-in takes the difference of the two signals, and multiplies it with the reference signal from the PEM driver. This results in a DC signal with an extremely high signal to noise ratio that corresponds to the polarization rotation induced by the cell. It can be shown that the relation between the output of the lock-in and θ is given by equation 6 (6).

$$\theta = \frac{\sin^{-1}\left(\frac{Vfr}{\sqrt{2}V_{DC}J_1(\beta)}\right)}{2} \qquad \text{eq. (6)}$$

Where Vfr is the output from the lock-in amplifier, β is the depth of retardation in radians, and V_{DC} is the summed output from the two photo detectors. The validity of equation 6 was verified by changing β, which resulted in no change in θ. Because the Bessel function is nonlinear, this is fairly conclusive evidence that this is an accurate relationship between θ and Vfr.

After solving equation 3 for [Rb], it takes the form shown in equation 7 with the ratio of rotation versus magnetic field. This ratio was obtained by measuring the slope of the line from a plot of θ versus B.

$$[Rb] = \frac{18\theta mhc}{Ble^2\mu_B}\left(\frac{\Delta^2_{1/2}\Delta^2_{3/2}}{4\Delta^2_{3/2} + 7\Delta^2_{1/2} - 2\Delta_{1/2}\Delta_{3/2}}\right) \qquad \text{eq. (7)}$$

IV. DATA AND RESULTS

As mentioned previously, the goals of this project were to measure the Rb vapor density, compare cell to cell variations, compare the Rb vapor densities against the Killian curve, and to check for long term changes. These measurements were made on the same three cells used by Ryan. These cells are listed in table 2. The lengths of the cells used in these measurements were slightly different than those used by Ryan. The overall lengths of the cells were measured with a digital caliper. The length of the inside of each cell was then estimated by subtracting off 1/8" for the thickness of each end cap.

Cell Name	Contents	Gas Pressure (mbar)	Length (cm)
120A	$^3He + N_2$, Rb	399	9.65
120B	$^3He + N_2$, Rb	750	9.47
120C	$^{129}Xe + N_2$, Rb	722	9.53

Table 2 Rb cells Used for Making Measurements.

The measurements were made by entering both the voltage across the main field resistor, and the voltage from the lock-in amplifier into an excel spreadsheet. Excel calculated the magnetic field strength by plugging this voltage into the main field slope equation in Figure 10. Excel then calculated the rotation by plugging the lock-in voltage

into equation 6. Rotation was plotted against magnetic field, and the slope was plugged into equation 7 resulting in a rubidium vapor density for a given temperature.

To check for hysteresis due to both B-field and temperature fluctuations, the field was ramped up and down at each temperature, and the temperature was ramped up and down for each cell.

The empirical formula developed by Killian for measuring the Rb vapor density is shown as equation 8 (2).

$$\log_{10} N = 26.41 - \frac{4132}{T} - \log_{10} T \qquad \text{eq (8)}$$

Where N is the Rb vapor density per cm^{-3}, and T is the absolute temperature. The measured vapor densities of cells 120A, 120B and 120C were compared to the Killian curve produced by equation 8.

At low fields, below approximately 10 gauss, the slope of rotation versus B-field is much steeper than that measured between 10 and 60 gauss. It is not clear what causes this dual slope behavior. However, because the slope obtained between 10 and 60 gauss was the one needed to make the calculation, all the data reported here was taken from that range. One other peculiarity was that the different cells absorbed different amounts of light. The same laser power was used on all the cells, however, the summed photo detector voltages were different for all the cells. This is shown in Figure 15.

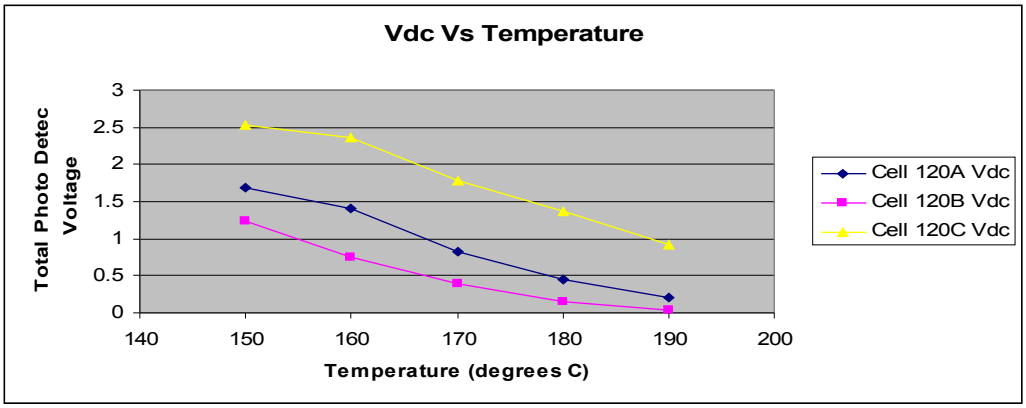

Figure 15 Shows the relationship between the total summed signal from the two photo detectors, and temperature. The plot indicates that different cells absorb different amounts of light, and that they all absorb more light with increased temperature.

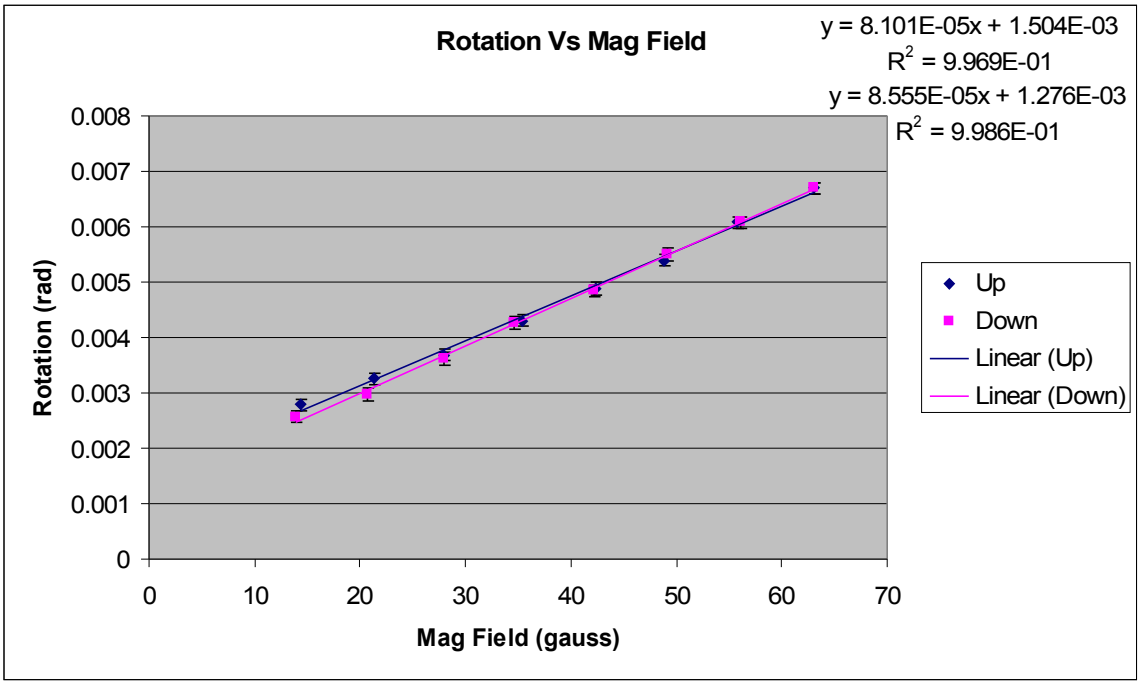

Figure 16 50707 Temp 150C Temp Up Cell 120A

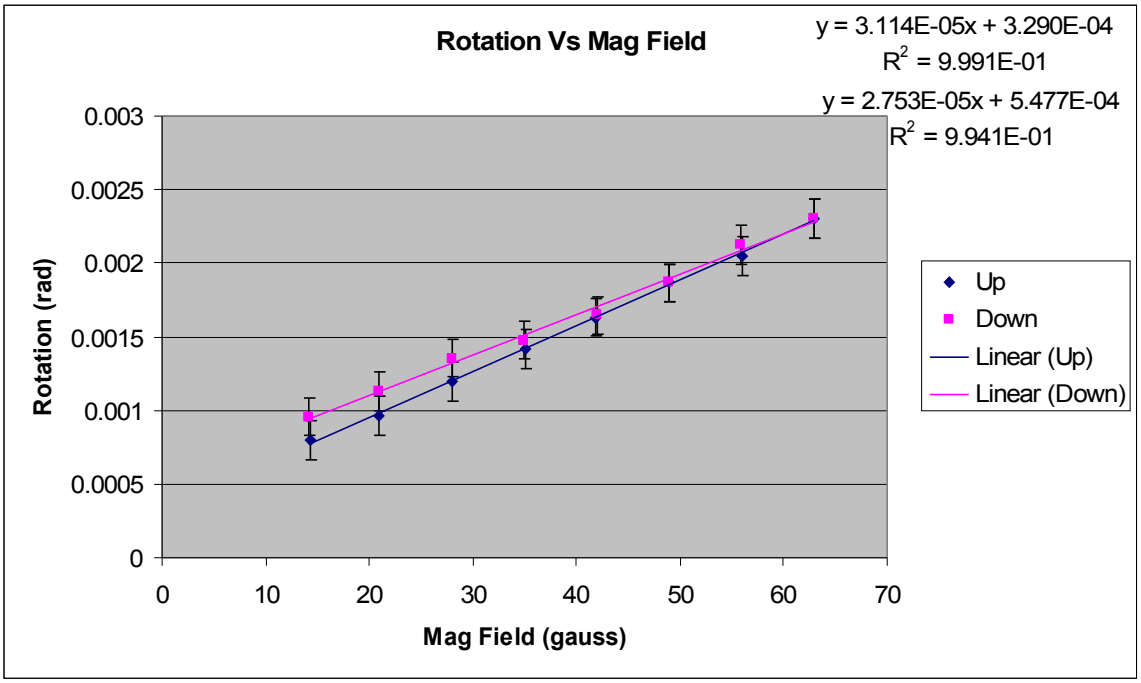

Figure 17 50707 Temp 160C Temp Up Cell 120A

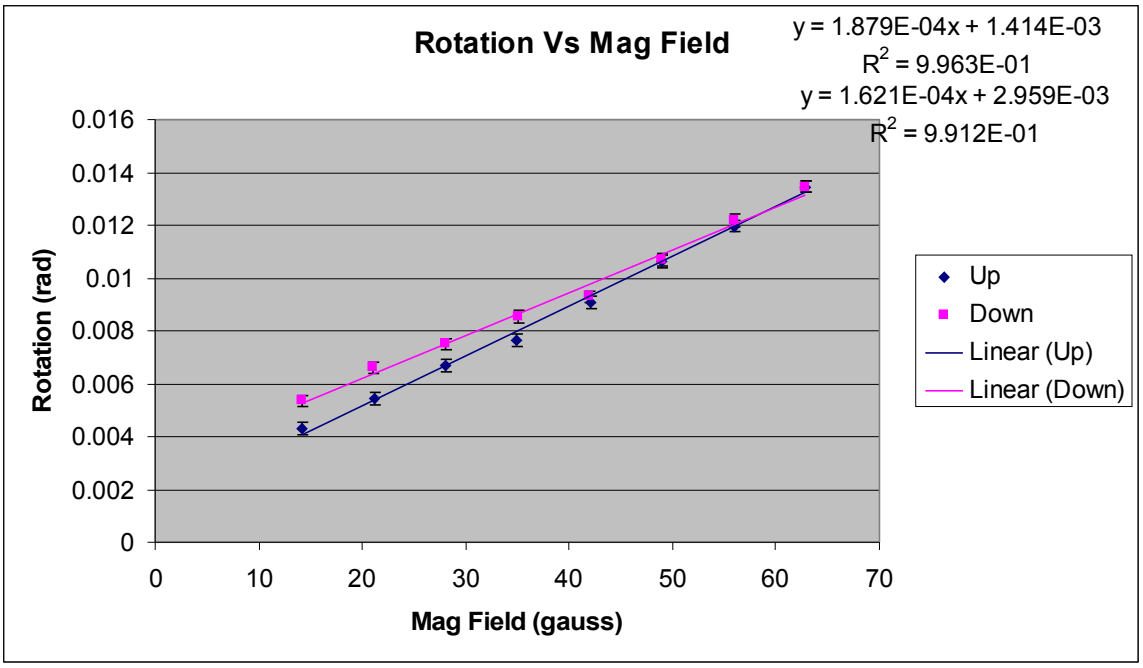

Figure 18 50707 Temp 170C Temp Up Cell 120A

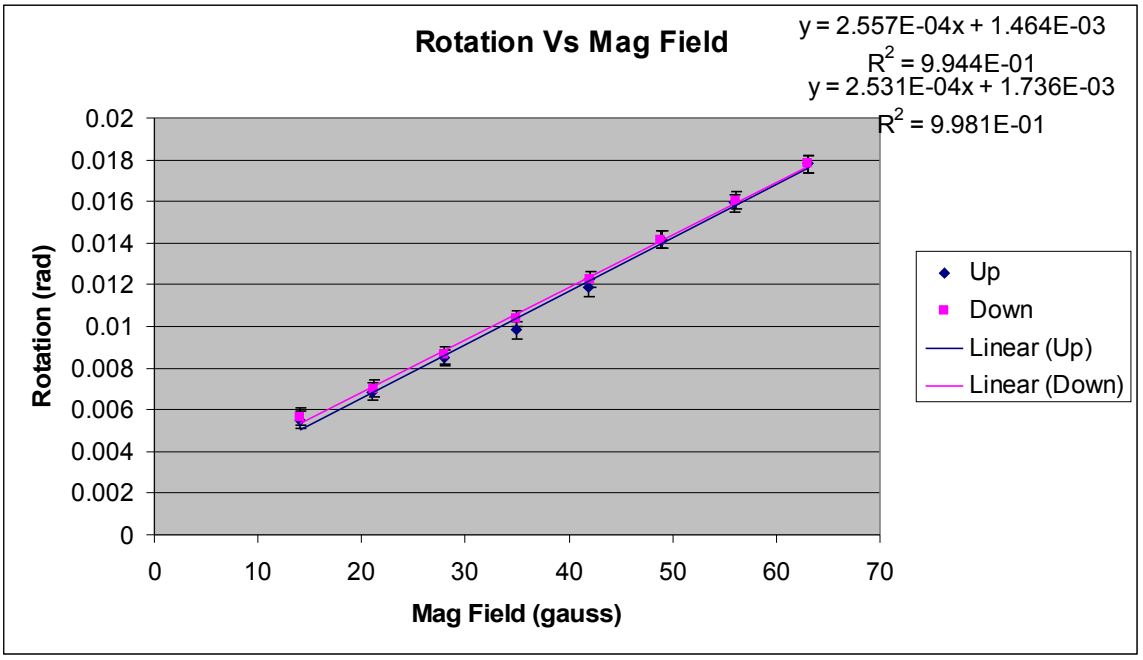

Figure 19 50707 Temp 180C Temp Up Cell 120A

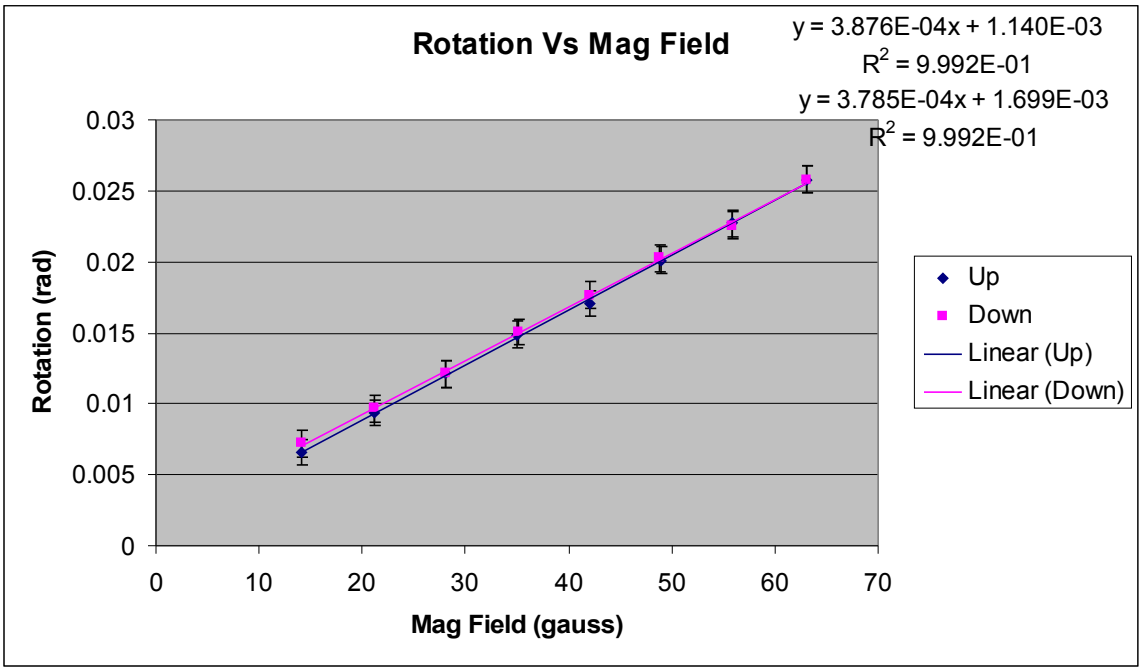

Figure 20 50707 Temp 190C Temp Up Cell 120A

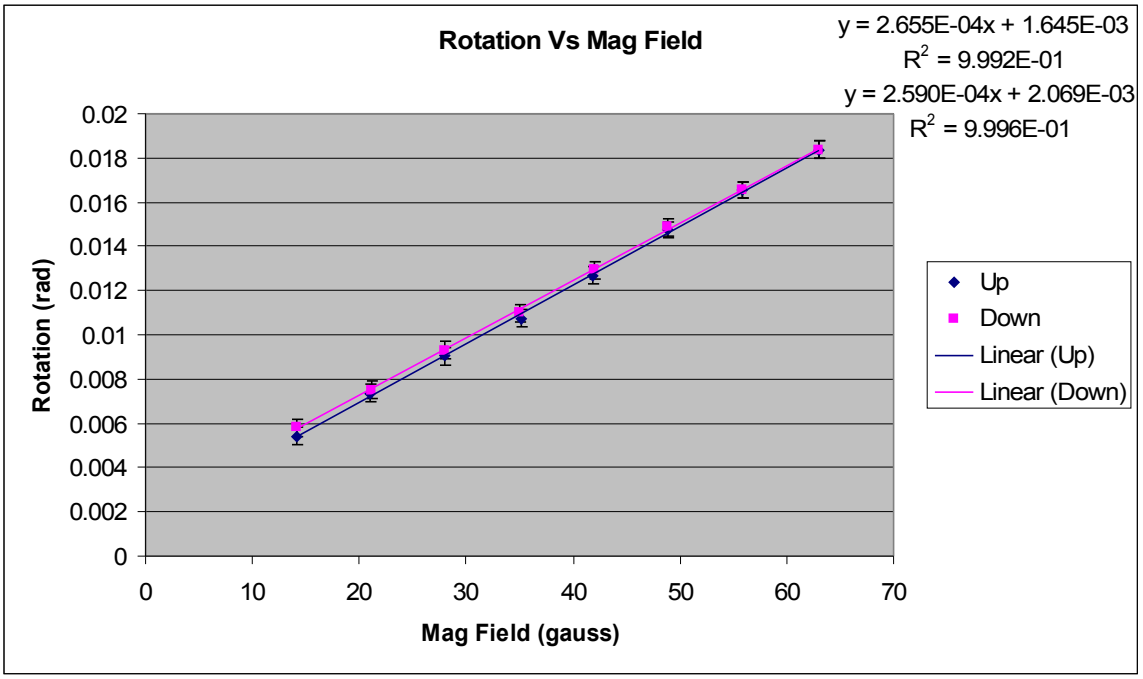

Figure 21 50707 Temp 180C Temp Down Cell 120A

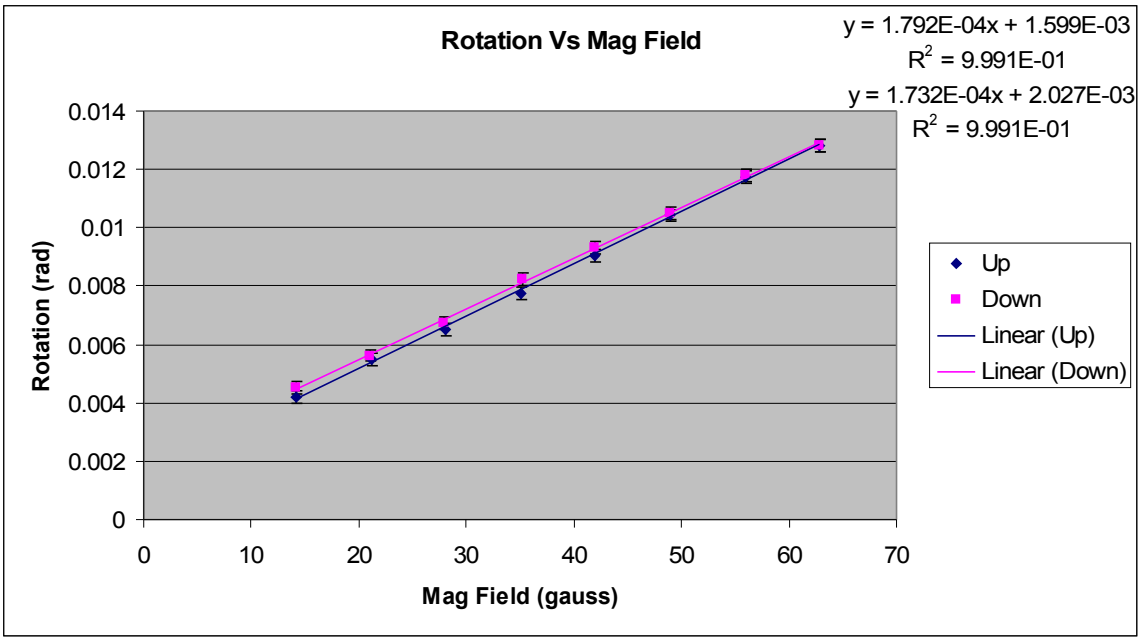

Figure 22 50707 Temp 170C Temp Down Cell 120A

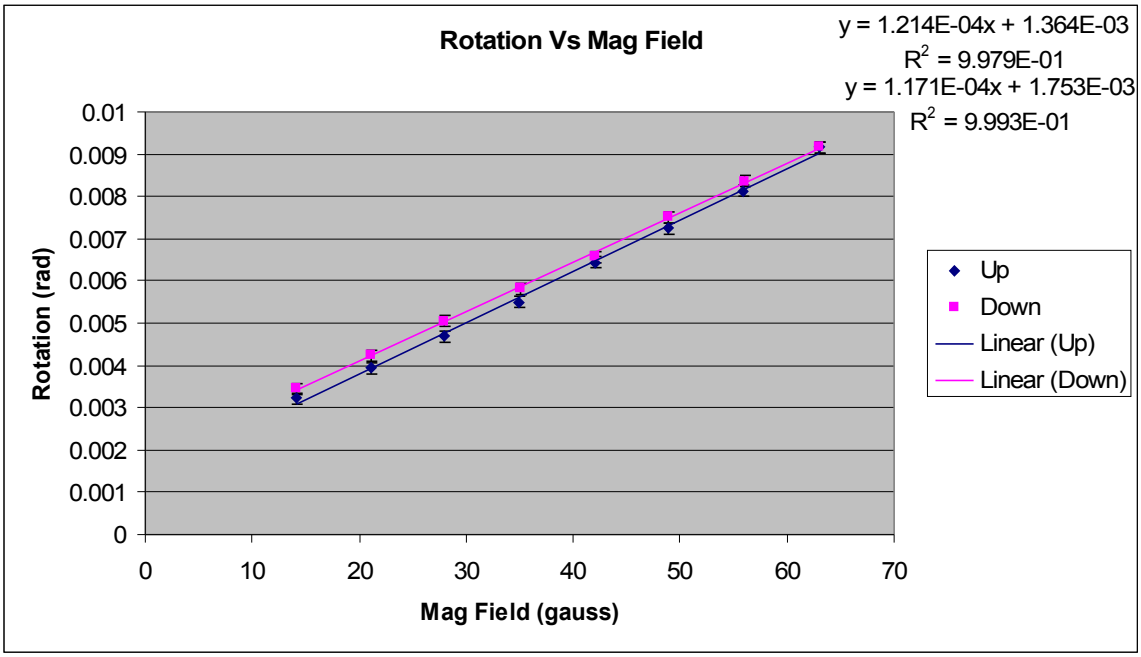

Figure 23 50707 Temp 160C Temp Down Cell 120A

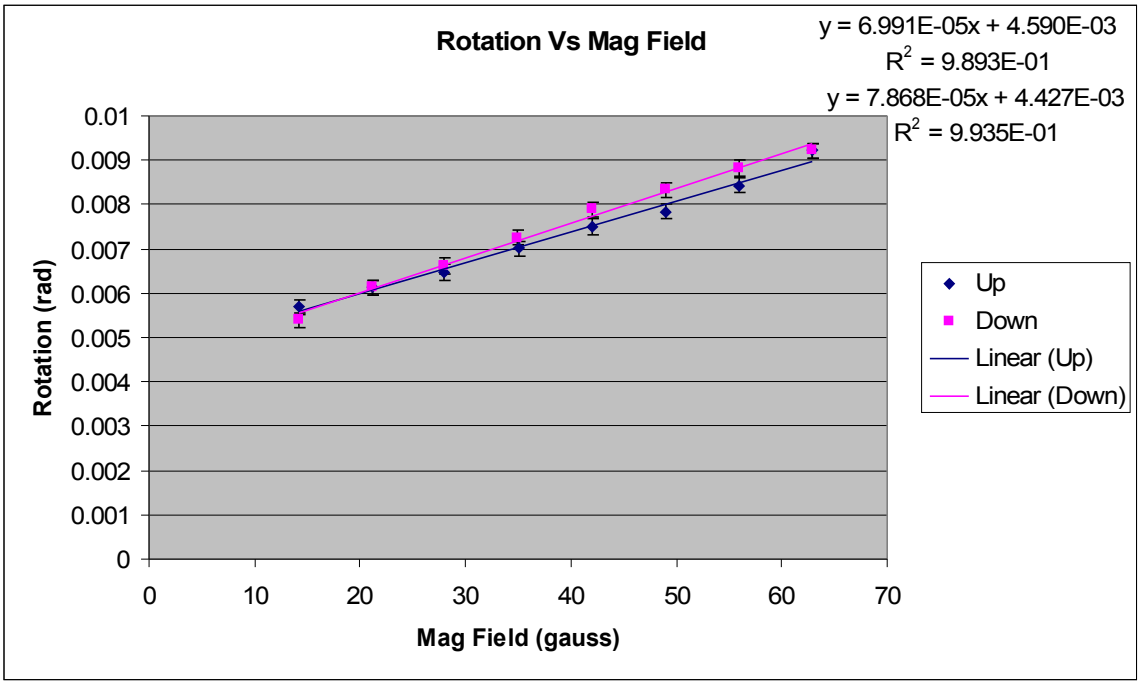

Figure 24 51107 Temp 150C Temp Up Cell 120B

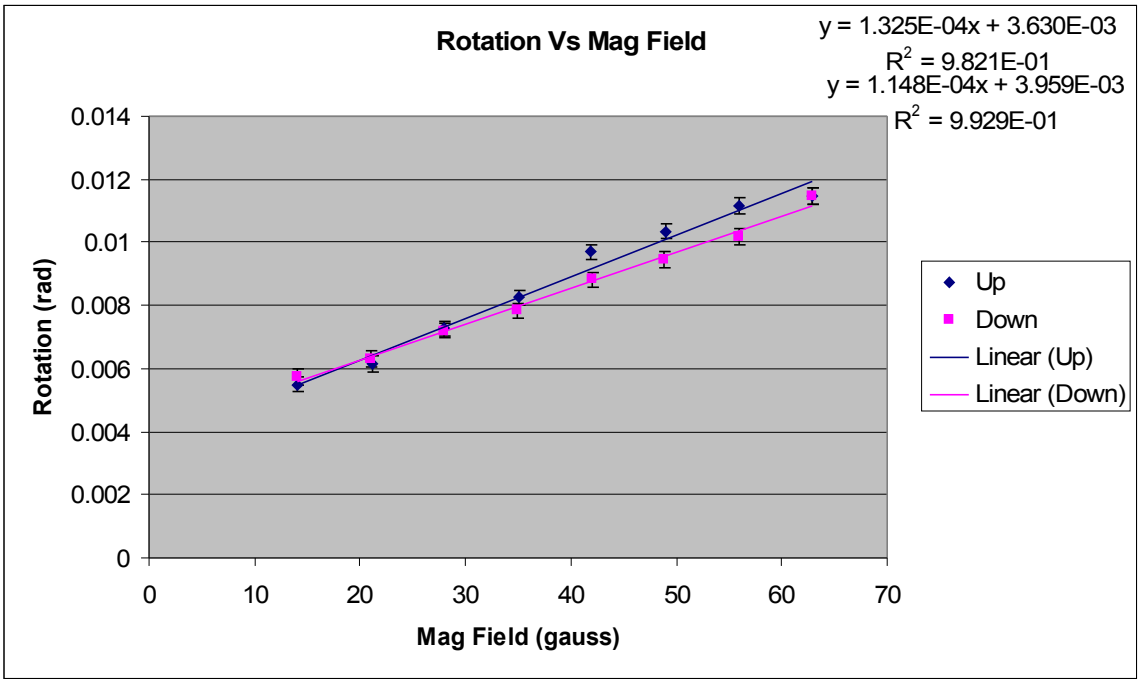

Figure 25 51107 Temp 160C Temp Up Cell 120B

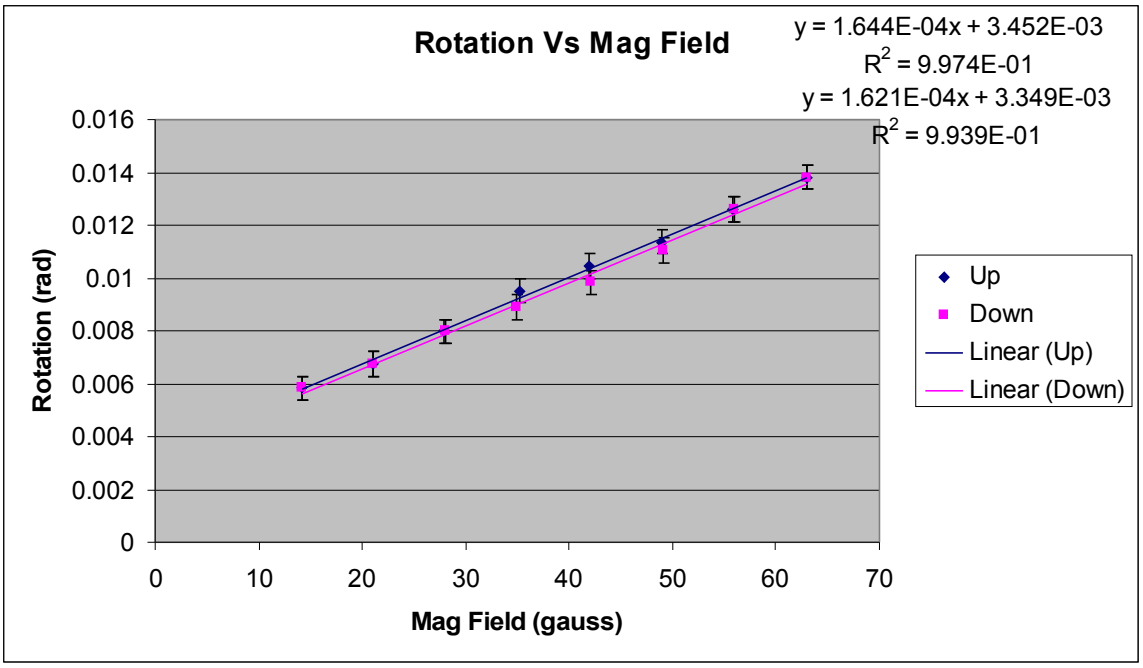

Figure 26 51107 Temp 170C Temp Up Cell 120B

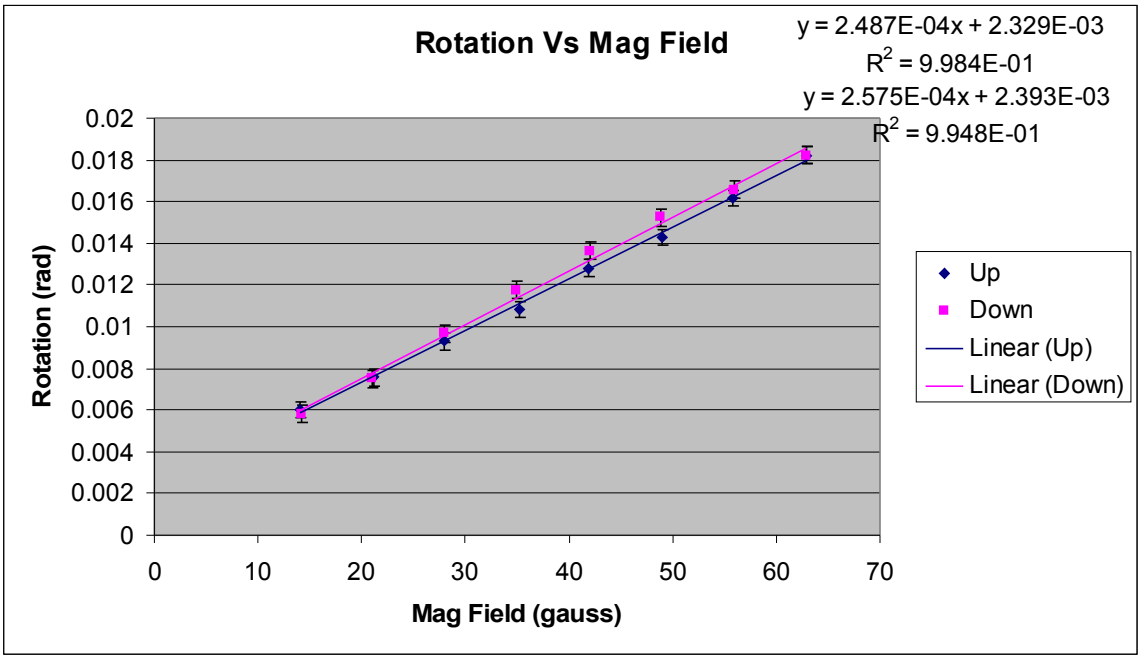

Figure 27 51107 Temp 180C Temp Up Cell 120B

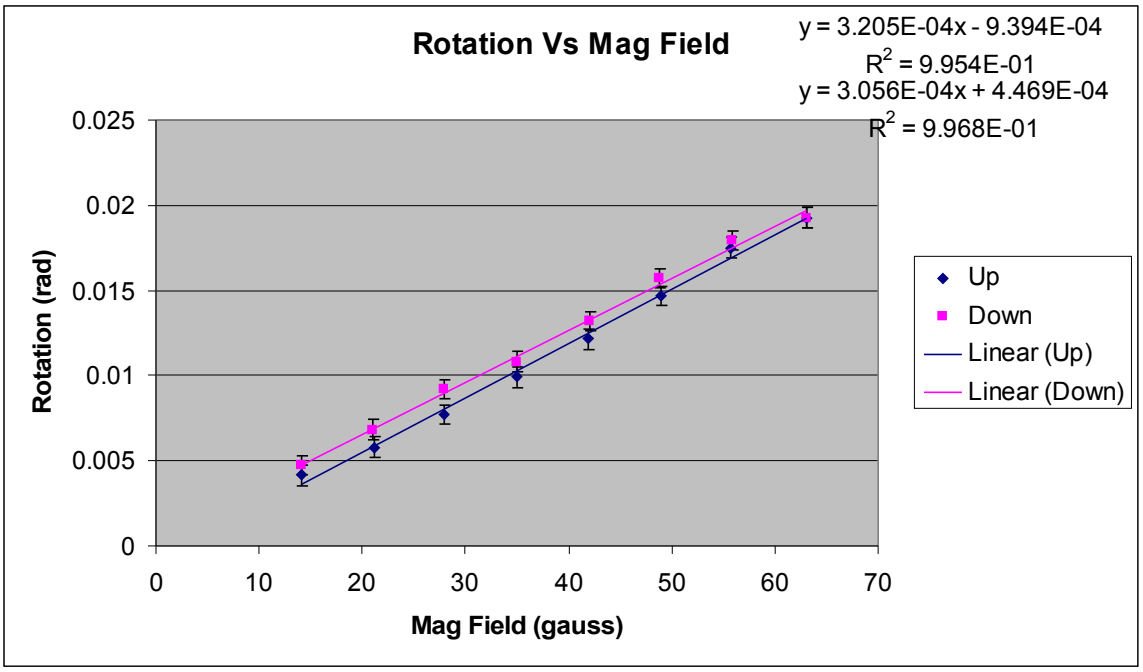

Figure 28 51107 Temp 190C Temp Up Cell 120B

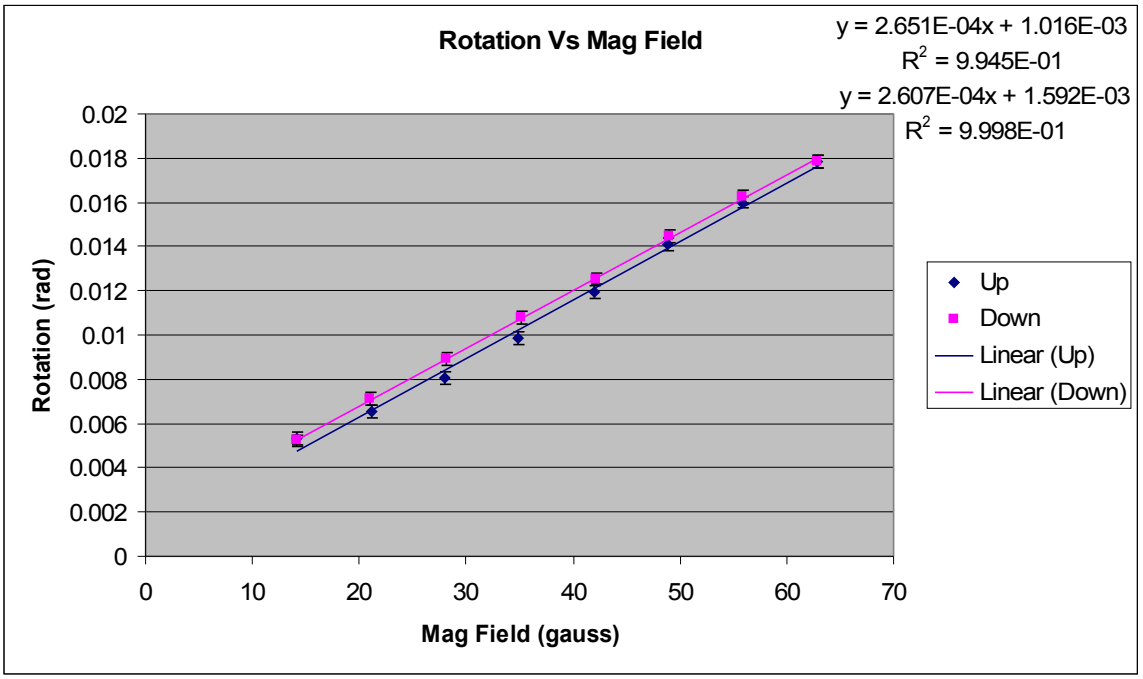

Figure 29 51107 Temp 180C Temp Down Cell 120B

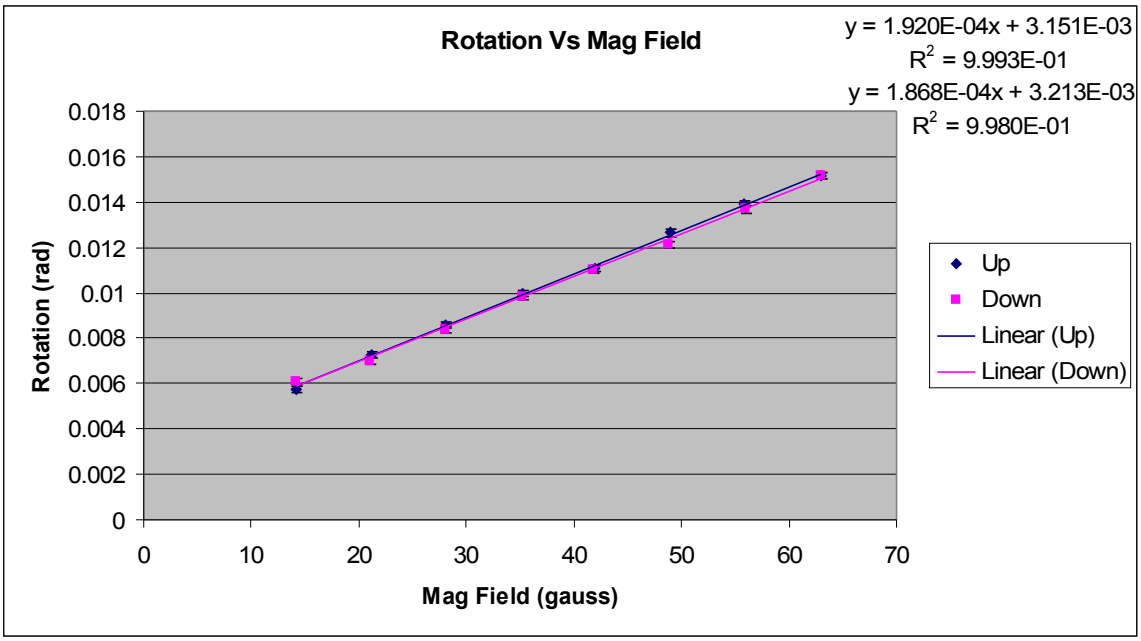

Figure 30 51107 Temp 170C Temp Down Cell 120B

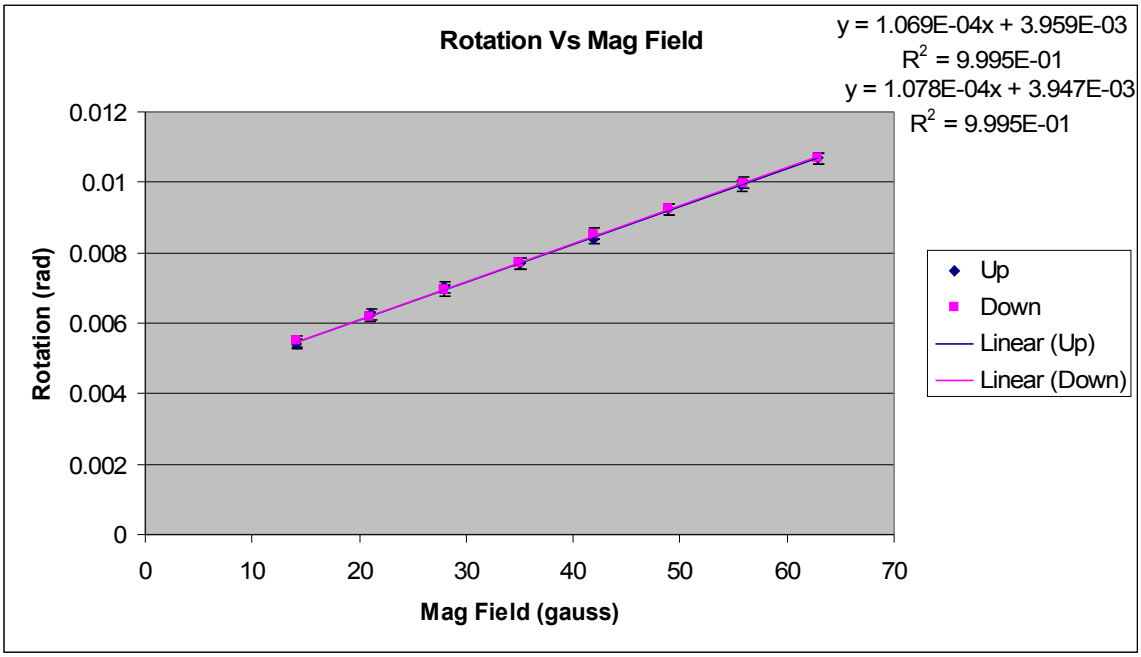

Figure 31 51107 Temp 160C Temp Down Cell 120B

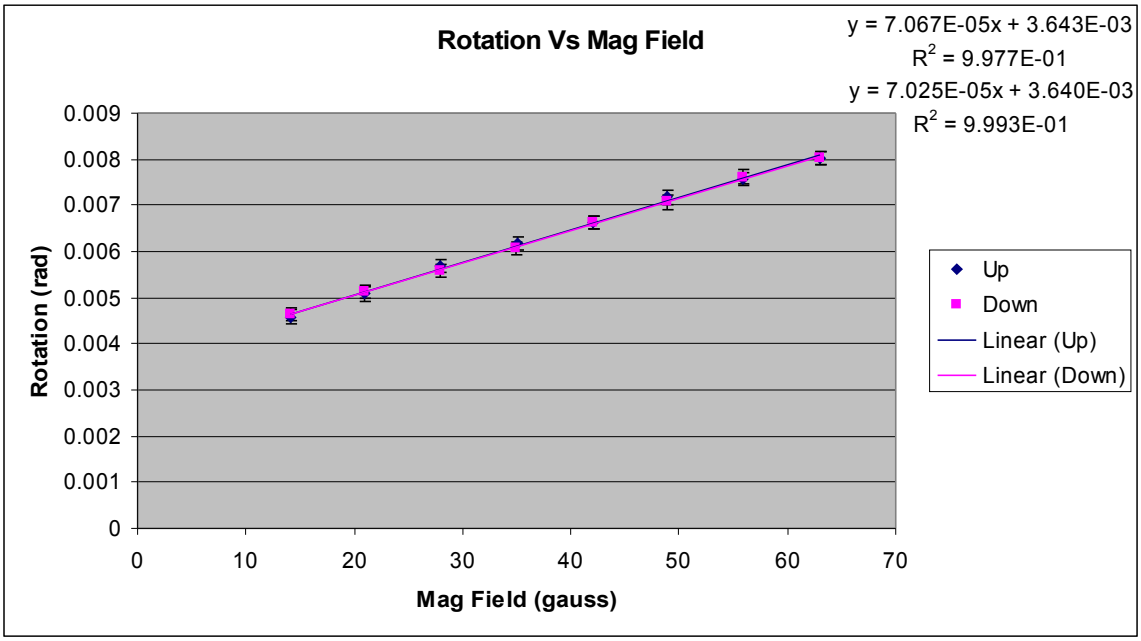

Figure 32 51107 Temp 150C Temp Down Cell 120B

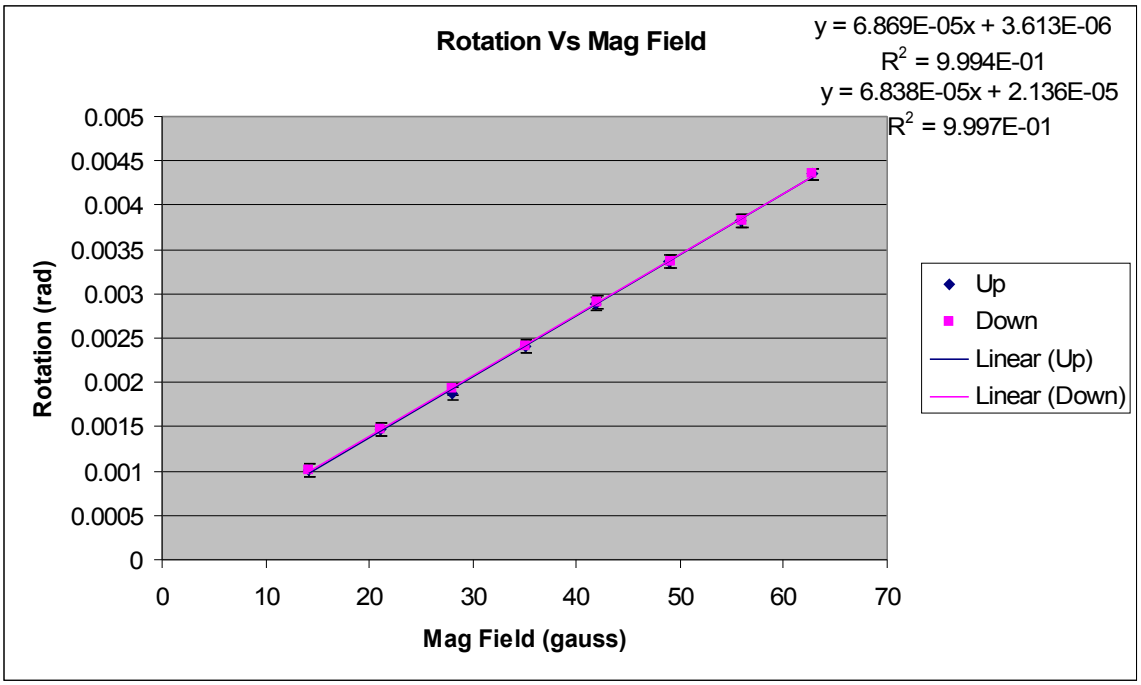

Figure 33 51407 Temp 150C Temp Up Cell 120C

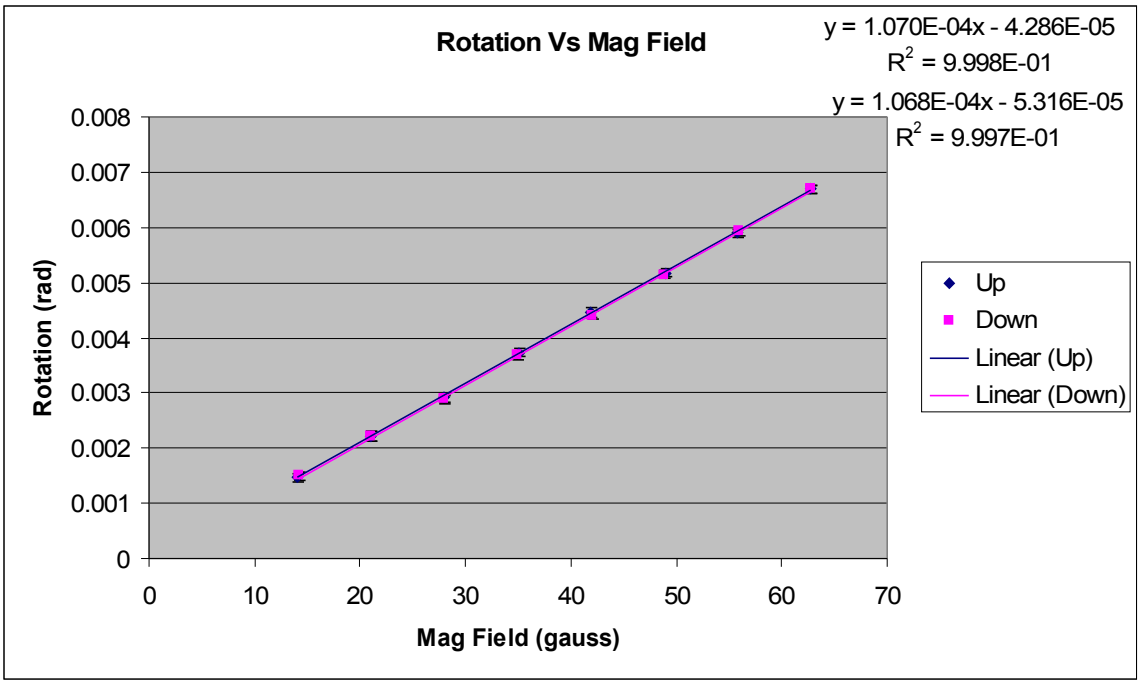

Figure 34 51407 Temp 160C Temp Up Cell 120C

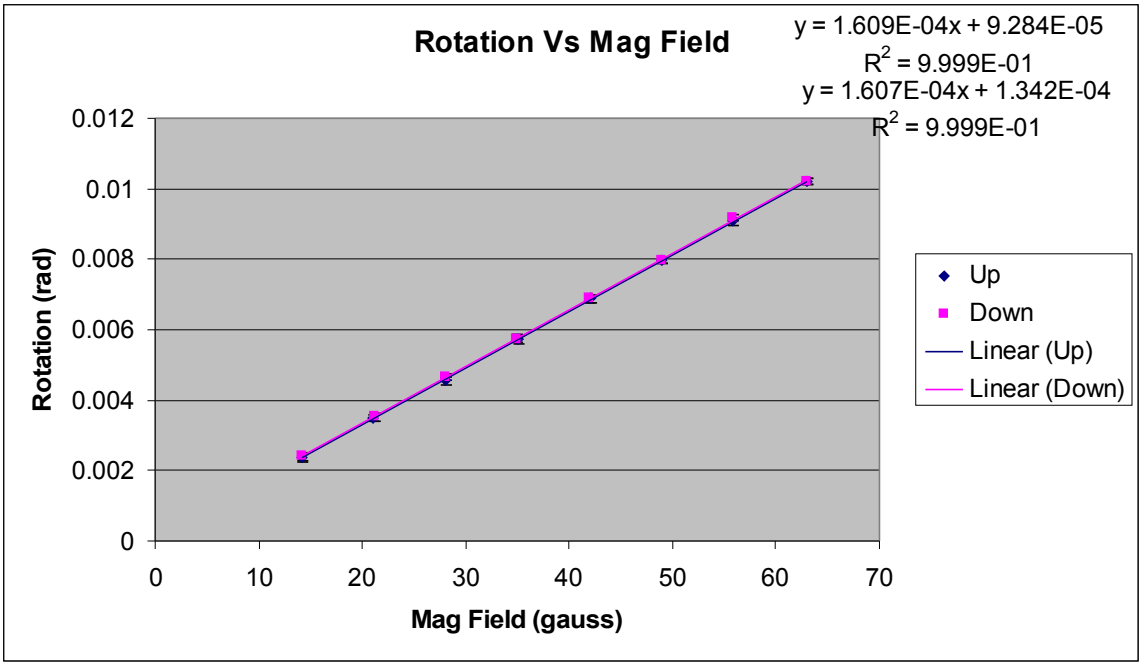

Figure 35 51407 Temp 170C Temp Up Cell 120C

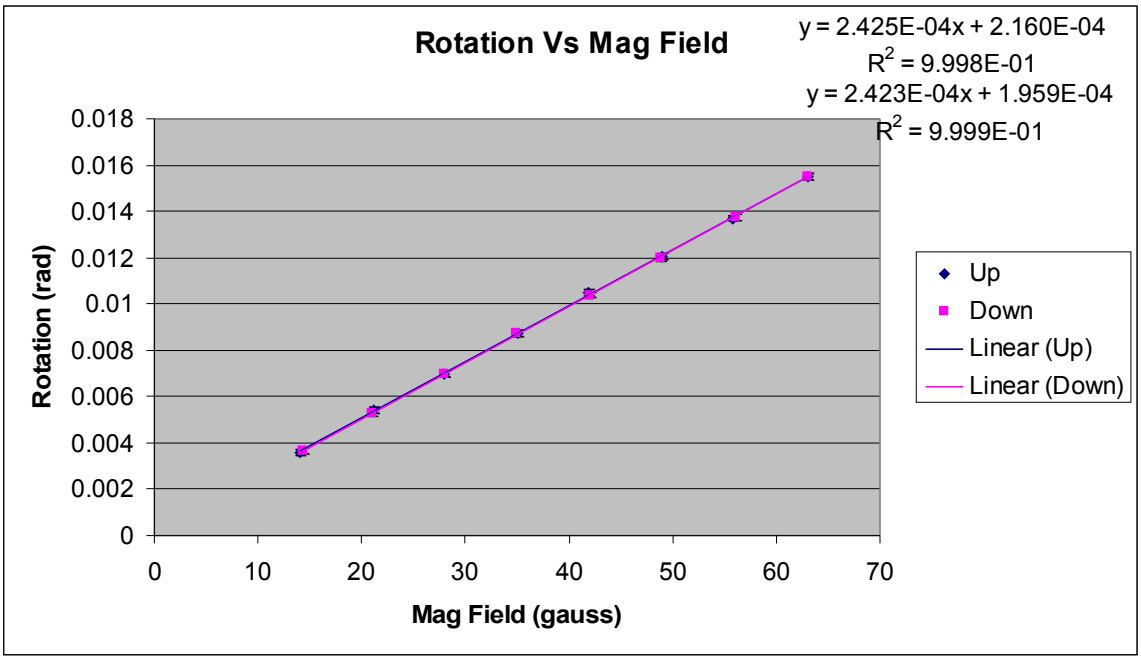

Figure 36 51407 Temp 180C Temp Up Cell 120C

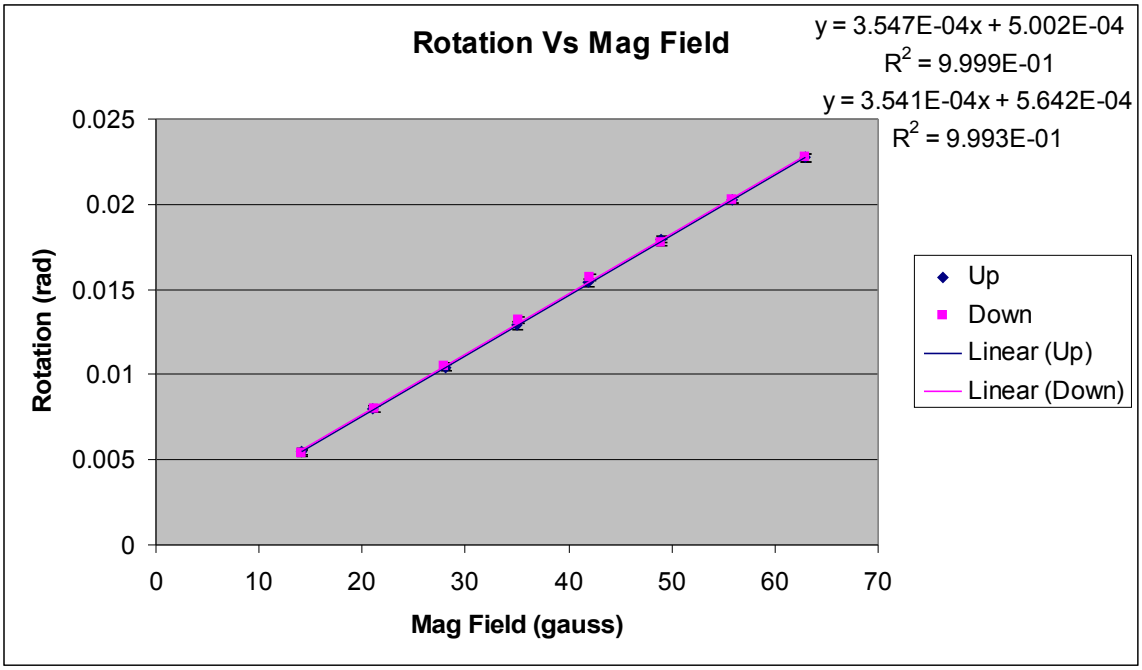

Figure 37 51407 Temp 190C Temp Up Cell 120C

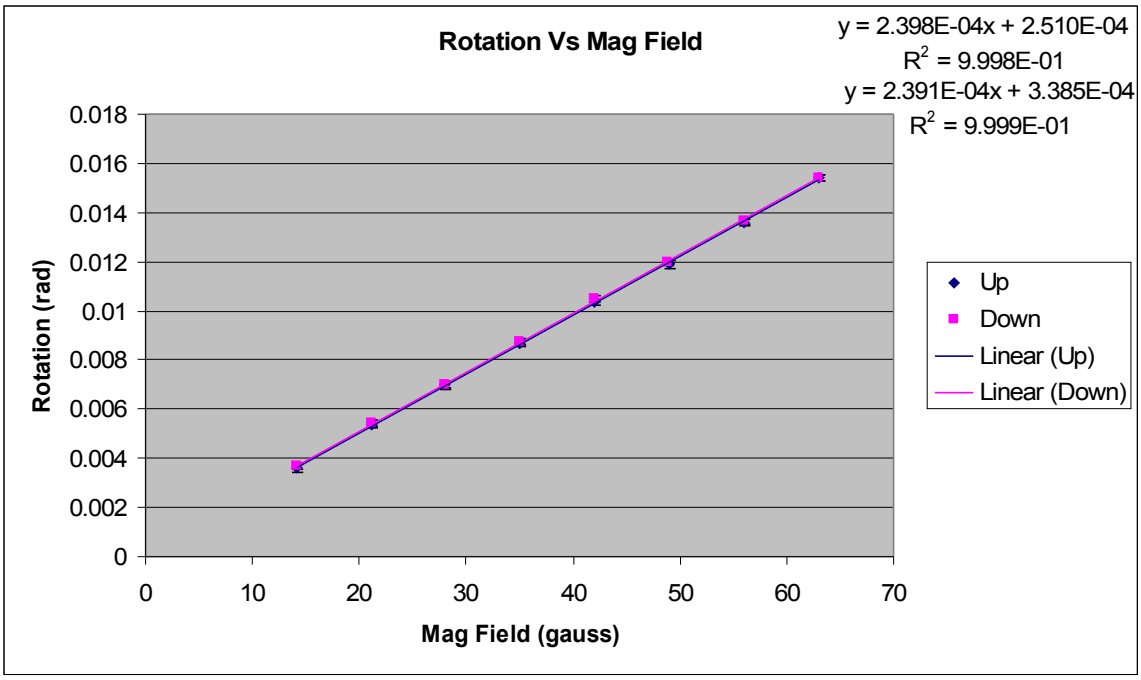

Figure 38 51407 Temp 180C Temp Down Cell 120C

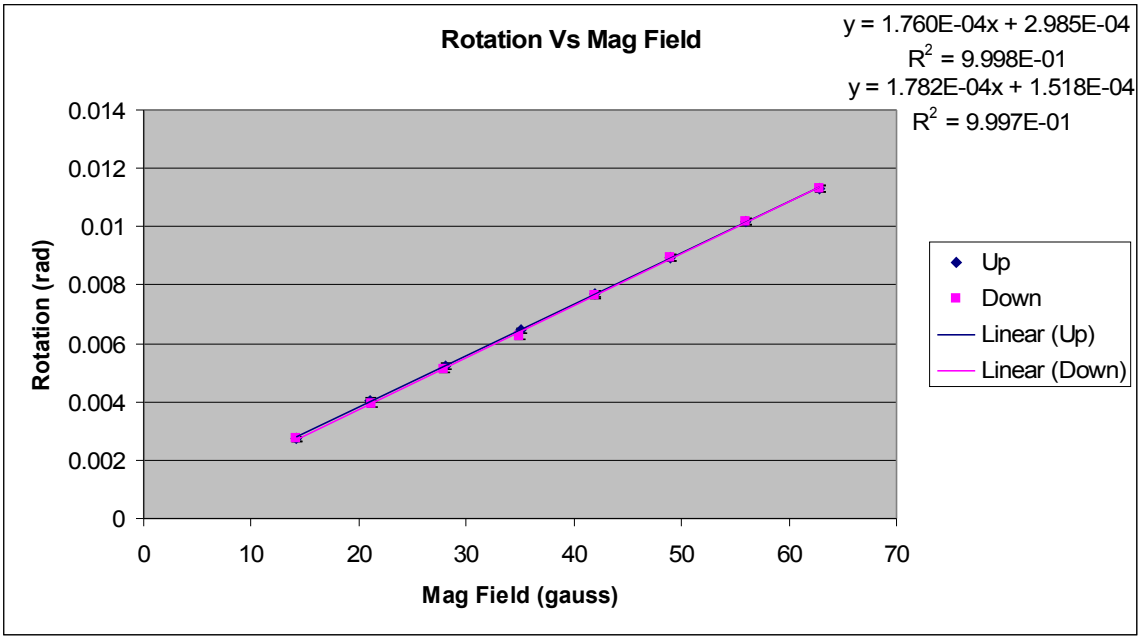

Figure 39 51407 Temp 170C Temp Down Cell 120C

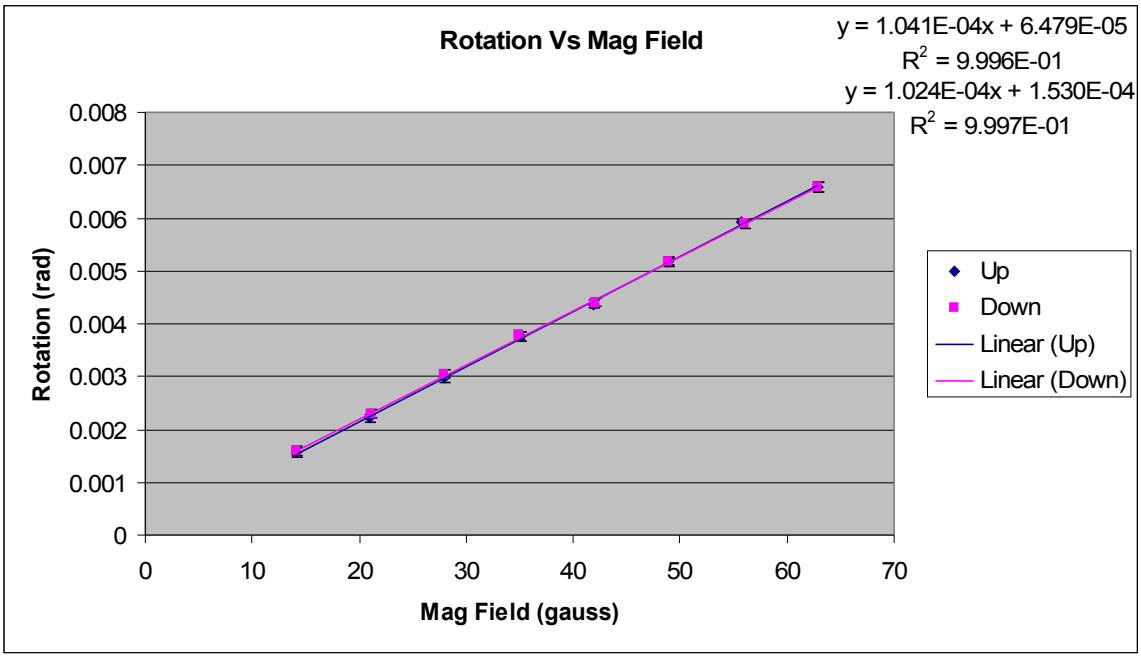

Figure 40 51407 Temp 160C Temp Down Cell 120C

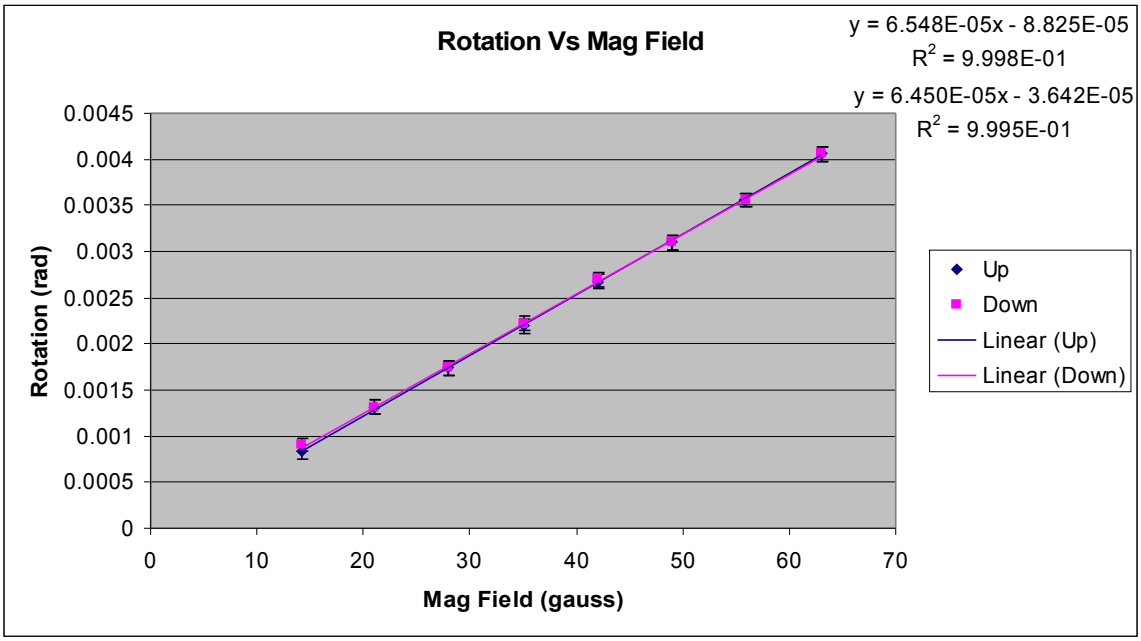

Figure 41 51407 Temp 150C Temp Down Cell 120C

Cells 120A and 120B show some signs of hysteresis do to changes in magnetic field. These cells were the first to be measured, and the frailties of the system were not completely understood at this point. It is believed that this apparent hysteresis may have been a result of laser power fluctuations causing the lasing line to vary slightly. The laser was believed to be more stable while measuring cell 120C which showed no sign of hysteresis. It has been determined through error analysis that for most of the measurements in this report, the error is dominated by frequency shifting, and not slope variations. However, the contributions to error from the frequency detuning, and the slope variations are both included in the error bars on the final [Rb] plots. Further tests are required to verify that there indeed was no hysteresis in cells 120A and 120B.

A comparison of the measured Rb vapor density and the Killian curve was made for each of the cells. These are shown in the following three figures. Each temperature has four data points. The four data points correspond to ramping the magnetic field up, ramping the magnetic field down, ramping the temperature up, and ramping the temperature down.

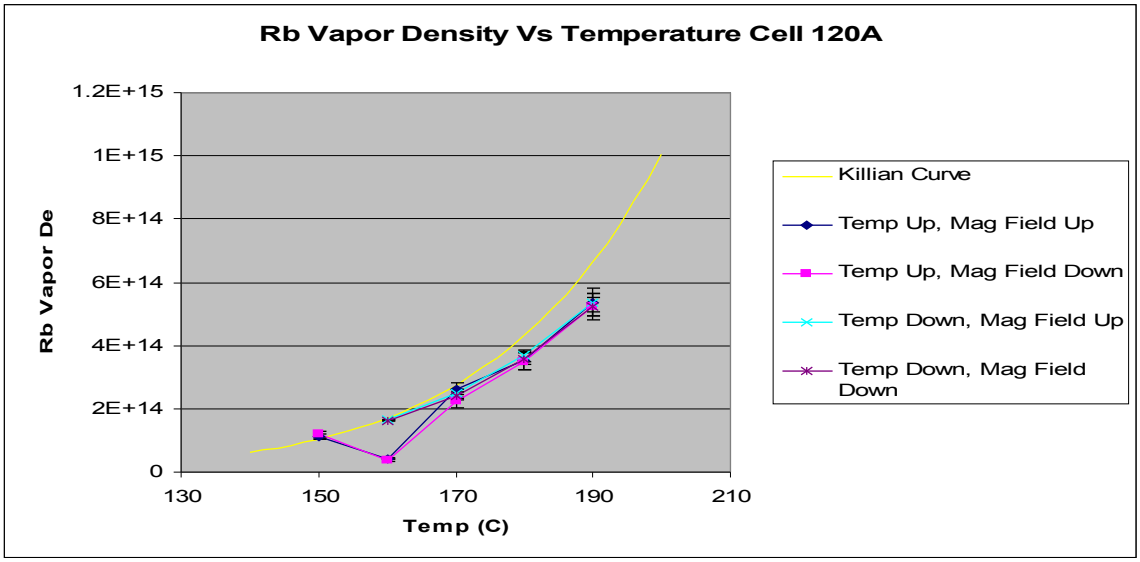

Figure 42 50707 Rb Vapor Density Cell 120A

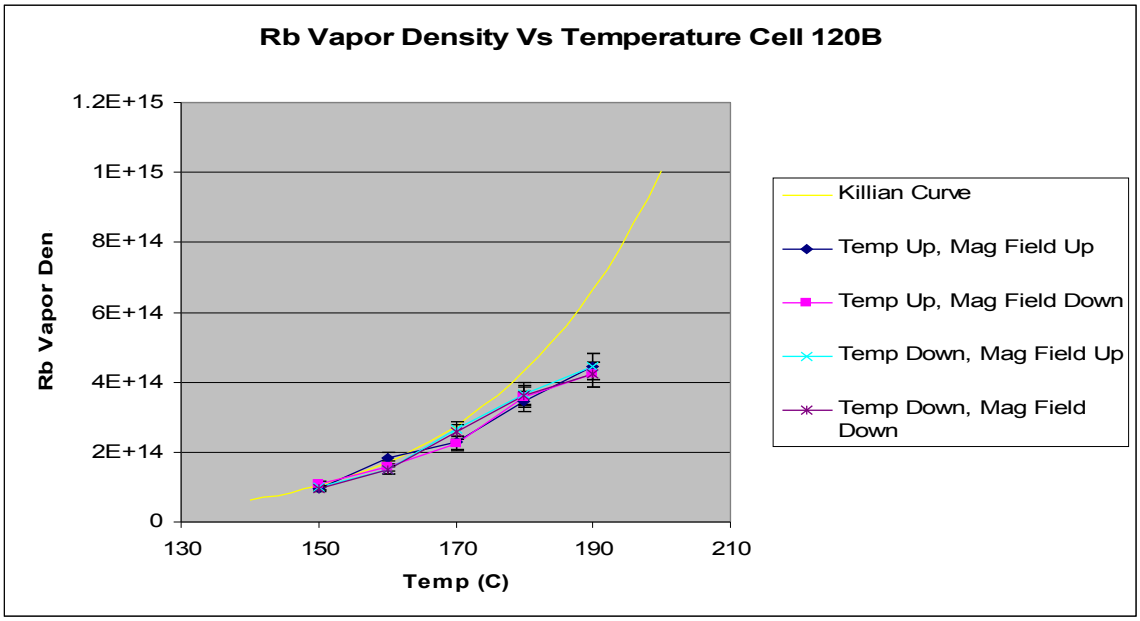

Figure 43 51107 Rb Vapor Density Cell 120B

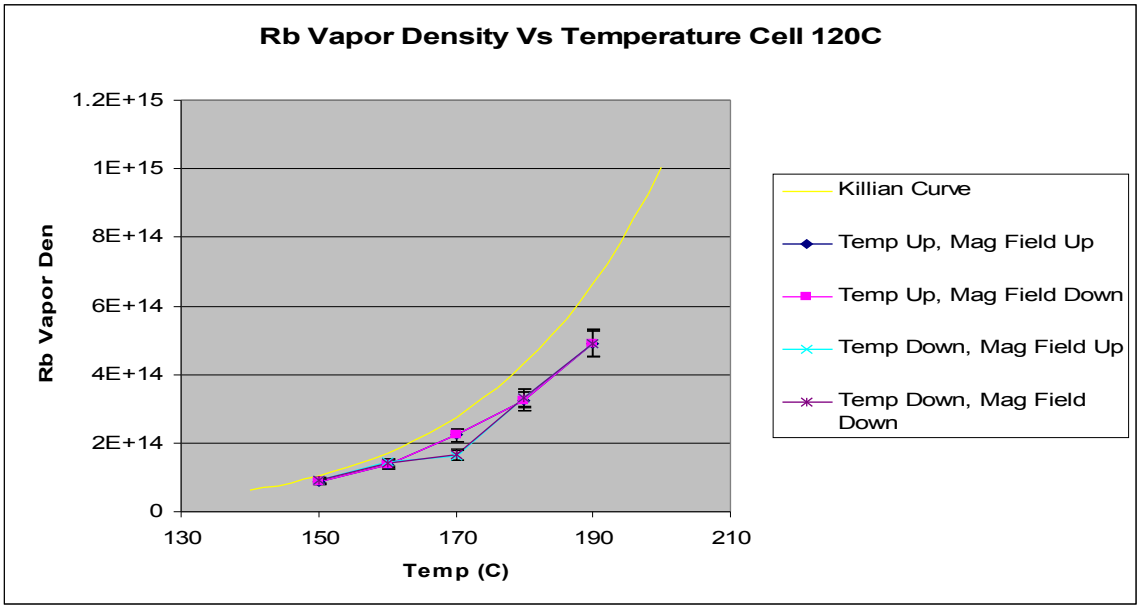

Figure 44 51407 Rb Vapor Density Cell 120C

All three cells showed the same trend of starting at the Killian curve for lower temperatures, and then deviating from the curve for higher temperatures. All three cells also deviated to the lower side of the Killian curve with cell 120B deviating the most at

190º C. Cell 120B was also the cell that absorbed the most light, therefore the increased deviation from the Killian curve may have been partially caused by low laser power.

A plot from Ryan's report is included in Figure 45 to show the improvement the PEM made for measuring the slope of rotation versus magnetic field.

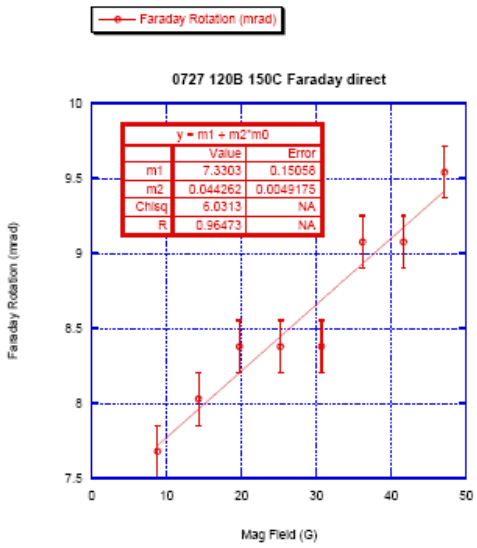

FIG. 17: Cell 120B, 150 °C; 47.4 mA laser current, $\lambda = 779.46$ nm

Figure 45 Plot from old instrument illustrating variance in the slope.

The plot shows much more deviation in the data points than those taken using the PEM. It is important to note that there are three points of introduction of error into the final [Rb] equation, the slope, the length of the cell, and the detuning. In this study, the length of the cell was not found to contribute a significant portion of the error and was not included in the analysis. Ryan reported a final error of ~10%. However, he also used a detuning variance of 0.01nm which results in ~4% error. This indicates from equation 9 that ~9% of his error came from the slope. Where the S term is the percent of slope error, and the q term is the percent of detuning error.

$$\frac{\delta N}{N} = \sqrt{\left(\frac{\delta S}{S}\right)^2 + \left(\frac{\delta q}{q}\right)^2} \qquad \text{eq. 9}$$

Being that the cursor resolution on the spectrometer is 0.04 nm, it is in my opinion that 0.01 nm is not a sufficient detuning variance. Therefore 0.02 nm or 8% error was chosen for the detuning variance for this error analysis. In this report, typical total errors for the

rubidium vapor density were ~8% to 9%. This is not much better than 10%, however, very little portion of the total error came from the slope measurements. Most of the total error comes from detuning which is estimated to be higher in this report than in Ryan's. This shows that the error coming from the slope has been significantly reduced by adding a PEM and lock-in amplifier to the instrument.

For all the measurements made in this report, a polarizer was placed directly after the laser. This was to ensure that all the laser light was vertically polarized. After the series of measurements was taken for this report, the polarizer was removed. Taking additional measurements showed that the error introduced by not having the polarizer in the setup was small compared to the error from the laser detuning. In fact, most of the error comes from laser instability. Laser instability is particularly noticeable when making the summed photo detector measurement. The voltage would change by about 10% very erratically. This can be fixed by ensuring the photo detectors are properly aligned, by adjusting the current on the laser power supply, and by adjusting the top knob on the ECDL shown in figure 3. To keep from damaging the polarizer used in the set up, a relatively modest laser current of about 38.7 mA was used. It might be advantageous to increase the laser power, especially in the case of cell 120B where so much of the light was absorbed.

IV. CONCLUSION

Rubidium vapor density measurements were successfully made using the photoelastic modulator and lock-in amplifier. The strong linearity of rotation as a function of magnetic field, especially for cell 120C, indicate that the employment of the PEM and lock-in amplifier have significantly increased the sensitivity, and reduced the error when compared to the previous setup. When compared to the Killian curve, the measured Rb vapor densities tend to follow the general form of the curve, with increasing deviation for higher temperatures. Unfortunately, because of time constraints, long term measurements were not feasible for this study.

Comparing the cells against each other indicate some variation from each other. Cell 120C deviated from the curve faster than the other two. Cell 120C also absorbed the least amount of light which may be correlated to the increased deviation. The variation in

cells indicates the necessity to be able to character each cell individually instead of relying on the Killian formula.

There was some slight hysteresis observed for cells 120A and 120B for variations in the magnetic field. Because cells 120A and 120B were the first to be measured, it is not clear if some of the apparent hysteresis was due more to inexperience in running the instrument, or was characteristic of the actual cells themselves. Further testing is recommended to verify this. Except in the most extreme cases, the error in the slope is dominated by detuning error. Therefore hysteresis due to changing magnetic fields, have negligible impact on the final Rb vapor density measurement. Hysteresis due to varying the temperature also appears to be negligible. Except for some outliers, the cause of which is believed not to be hysteresis, all the points for a given temperature agree with each other within experimental error.

APPENDIX A: OPERATIONS MANUAL

This operations manual does not cover the operations of the entire instrument. Rather, it only covers the operations of additions made to the instrument that Ryan May already made. For operations regarding the ECDL and the temperature controller for the ECDL refer to Ryan May's project report.

1. Using the Quarter Waveplate

With only the components shown in Figure 46, confirmation of best circular polarized light can be obtained by following the procedures listed below.

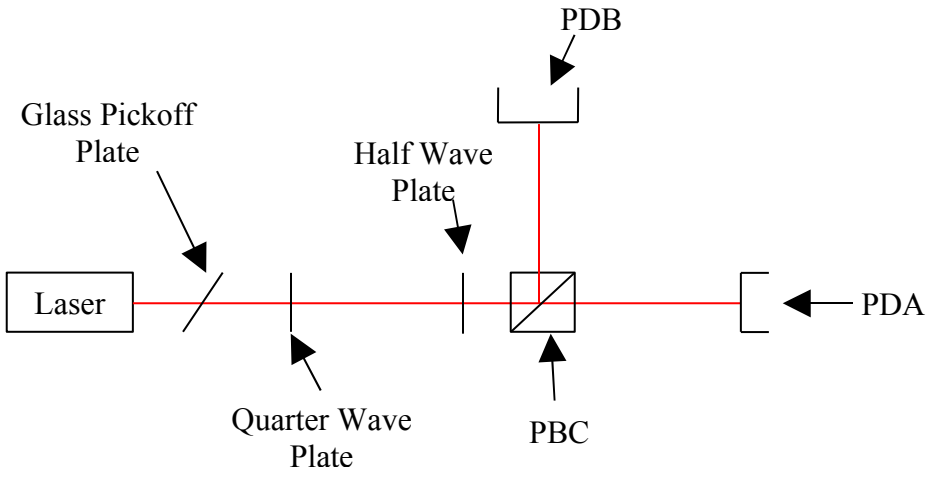

Figure 46 Setup used for producing best circular polarized light.

1. Rotate the quarter waveplate, so both the fast and slow axis are oriented 45º with respect to the laser beam polarization. Either the fast or slow axis on the quarter waveplate corresponds very closely to zero degrees on the rotation stage.
2. The quarter waveplate should be mounted on a post that is inline with either the fast or slow axis.
3. Plug the outputs of PDA and PDB into an oscilloscope. Make sure both channels are on the same scale.
4. With the laser on, adjust the position of the photodiode detectors PDA and PDB so their signal is maximized.
5. Rotate the half waveplate and observe the fluctuations in the two signals on the scope.
6. Adjust the quarter waveplate to minimize these fluctuations as the half waveplate is rotated.

7. Now, minimize fluctuations more by making slight rotations of the quarter waveplate about the post that it is mounted on. This causes the optical path length of either the fast or slow axis that is perpendicular to the post to be lengthened, while not affecting the other axis that is inline with the post. If the fluctuations only get worse, try rotating the quarter waveplate by 90º so the fast and slow axis have swapped positions, and repeat the above procedure.
8. Continue to make slight adjustments to the rotation of the quarter waveplate about the laser beam, and about the mounting post until the fluctuations of the signals as a function of half waveplate being rotated have been minimized. The system is now adjusted to produce the best circular polarized light. Most of the remaining signal fluctuation is due to error in the half waveplate.

2. Using the PEM

Introduce the PEM into the system immediately after the quarter waveplate. The PEM causes the laser beam to be shifted vertically by about 1 cm. Therefore readjustment of the downstream optics is necessary.

Figure 47 The PEM driver, electrical head, and the optical head.

Operation of the PEM

1. **Warning, do not turn on the PEM unless the optical head and the electrical head are connect with the interconnect cable. Serious damage may result.**
2. Turn the power on with the power button located on the front bottom left corner of the PEM controller.
3. The wavelength adjustment (WAV) is automatically highlighted. To highlight the depth of retardation adjustment (RTD), simply push the blue down button located on the right front face of the PEM controller.
4. With WAV highlighted, the wavelength can be adjusted by pressing enter.

5. Now that the number is highlighted. Simply enter in the desired wavelength using the numbered keys followed by enter.
6. To adjust the depth of retardation, follow the same procedure.

3. Using the Lock-in Amplifier

The lock-in amplifier used was a Princeton Applied Research model 186A Synchro-Het lock-in amplifier. With the input A-B option selected, the lock-in amplifier takes the difference of the two input signals, and then multiplies that signal with the reference signal. The output is a DC signal that corresponds to the amplitude of the difference of the two input signals.

Figure 48 Lock-in amplifier used on this instrument.

Because the input signal is oscillating at 50 kHz, the input lowpass filter is set to max which is 100 kHz. Because the reference signal out of the PEM is 1f, the 1f reference signal mode is selected on the lock-in amplifier. The correct sensitivity was chosen by choosing one that used the biggest portion of the scale, without pegging the needle, for a Faraday rotation measurement. There are three scales the needle can be read from, depending on the sensitivity setting used. A typical sensitivity setting used was 20 mV. For this setting, the scale that goes up to 2 was used. The output time constant determines how much the needle fluctuates. Lower time constants allow the needle to fluctuate more rapidly. Typical time constants used were 0.3 and 1 second time constants. The phase adjusts the phase between the input and reference signals. It can be adjusted by 90º increments using the buttons, or continuously by turning the

phase knob. The output offset can be useful if you wish to adjust the starting point for the output needle. Be aware that the phase can only be checked with the output offset turned off. The dynamic reserve used was always 3k.

4. Magnetic Coils

The magnetic coils were each individually calibrated by measuring the magnetic field with a Hall effect probe, and comparing that to a voltage measured across a power resistor through which all of the coil current ran. Attached to the front of the cart where all the power supplies are located are three equations that relate magnetic field to the voltage measured across a power resistor for each set of coils. The shim coils use a dual power supply indicated in Figure 49.

Figure 49 Power supplies used by magnetic field coils. Also shown is the laser temperature controller.

To properly adjust the shim coils for zero field, simply solve the appropriate equation for V(0). Then connect the magnetic field output voltage to the DVM located on the instrument cart as shown in Figure 50. Switch the selector switch to the correct coil, and adjust the current on the correct power supply until a voltage output is displayed that corresponds to zero field for that coil. Do this for each of the shim coils.

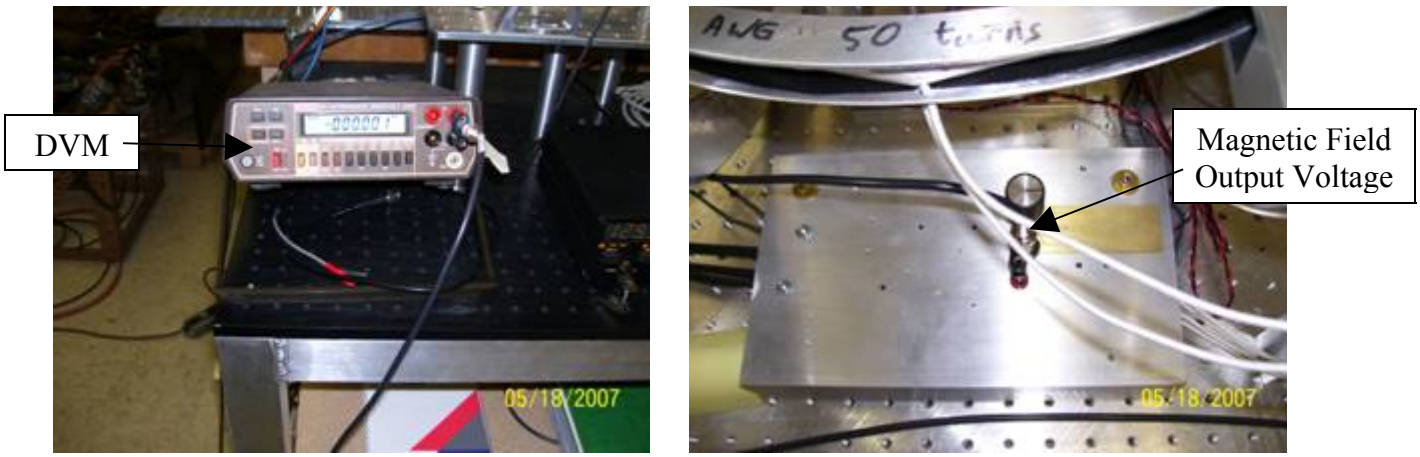

Figure 50 DVM and coil selector switch used to measure the magnetic field contribution for each of the three coils.

Adjusting the main field coils is the same as adjusting the shim coils except that there are two power supplies involved. The two power supplies are connected in a master/slave configuration with the master on top. To adjust the main field, turn both power supplies on. All the knobs on the slave power supply should be turned completely clockwise so both the voltage and current settings are maximum. The voltage knobs on the master power supply should also be set to their maximum position. The current control knob on the master power supply is then used to adjust the current output of both power supplies. When zero magnetic field is required, it is necessary to completely turn off both of the power supplies used for the main field coils. When the power supply is left on with the current turned all the way down, there is still a small current that results in Faraday rotation.

5. Making Measurements

Measurements can be made by following the list of instructions below.

1. Set the oven to the desired temperature and let it stabilize. Once it is stable, it should fluctuate by only ±0.3º C.
2. Turn on the shim coils, and verify with the DVM that they are adjusted to result in zero field in the oven space.
3. Turn the laser on.
4. Use the Ocean Optics spectrometer to measure the real time lasing wavelength. Adjust the ECDL if necessary.
5. Plug the output from photodetectors into the oscilloscope.

6. After all the optical elements are in place, including the oven and cell, adjust the photodetector positions to produce a maximum signal.
7. Turn on the PEM.
8. Plug the output from the photodetectors into the lock-in amplifier.
9. Switch between 0º and 90º, and adjust the phase knob so one of the positions (either 0º or 90º) gives zero signal. This means that the entire signal is on the other position or channel. Go to the channel with the entire signal.
10. With the main field power supplies turned off, rotate the half waveplate until the signal on the lock-in amplifier reads zero.
11. Open up the Excel file labeled RbDensityTemplate3.xls, and select the tab that corresponds to the correct temperature.
12. All the columns with bold inputs require user input, all the other columns are either constants or outputs, and do not need to be changed.
13. Plug the output from the photodiode detectors into the summer and plug the output from the summer into the oscilloscope.
14. Enter the summed voltage into the Vdc column overwriting the existing data.
15. Plug the photodetector outputs back into the lock-in amplifier.
16. Set the magnetic field selector switch to observe the main field.
17. Turn the main field power supplies on and adjust the current so the DVM reads ~400 mV. Input the exact voltage into the VB column.
18. Read off the voltage on the lock-in amplifier, and input this value into the column labeled Vfr.
19. Repeat steps 17 and 18, incrementing the magnetic field voltage by 200 mV each time, until a maximum of 1.800 V is reached.
20. When finished, Excel will output a [Rb] vapor density point.
21. Columns “B” and “V” are uncertainties or variance in the signal from the lock-in amplifier, and the Ocean Optics spectrometer respectively. They are used in the error calculations.
22. Repeat steps 1-21 for each temperature.

REFERENCES

[1] E. Hecht. *Optics, 4th ed.* Addison-Wesley, Reading, MA, 2002.

[2] R. May, Instrumentation Project Final Report, University of Utah, Utah, 2006.

[3] R. A. Serway, J. W. Jewett, *Physics for Scientists and Engineers, 6th ed.* Thomson Brooks/Cole, 2004

[4] PEM100 User's Manual, Hinds Instruments, 2006.

[5] K. C. Hewitt, Department of Physics and Atmospheric Science, Phys3540 Lecture, Dalhousie University, Halifax, Nova Scotia 2002.

[6] I. A. Nelson, Thesis, University of Wisconsin-Madison, 2001.

[7] T. J. Killian. Thermionic phenomena caused by vapors of rubidium and potassium. *Physical Review,* 27:578-587, 1926.

[8] B. Chann, E. Babcock, L. W. Anderson, T. G. Walker. Measurements of ^{3}He spin-exchange rates. Physical Review A, 66:032703, 2002.